Chapter III. Nonlinearity effect

Introduction

Le Claire's relation is still remaining the only one used for the evaluation of GB diffusivity (D_{gb}) from the diffusion profiles measured under conditions of type-B kinetics. The relation is based on the finding of Levine and McCallum [Lev60] that the GB part of $\ln C_{av} = f(y^{6/5})$ plot is a linear function. However, it is very difficult to suggest a scale in which the diffusion profile is exactly a linear function for a broad range of parameters. In this chapter we investigate the validity of such a linear dependence for short diffusion times.

3.1 Important definitions

For that purpose Whipple's solution was integrated, fixing the penetration depth at 500 nm and varying the diffusion time (t) and the ratio of diffusivities (Δ). These are the typical experimental conditions [Mis99] too when measuring the concentration profile and determining the GB diffusivity (D_{gb}), because Δ is unknown. For the integration a sample characterized by a width of 25 nm and a length of 500 nm was used. Such a sample is called

hereafter also as a geometrical model. The value for $D_g = 2.95 \cdot 10^{-4}$ nm^2/s ($2.95 \cdot 10^{-16}$ mm^2/s) as well as $D_{gb} = 6.42$ nm^2/s ($6.42 \cdot 10^{-12}$ mm^2/s) were taken from the Arrhenius relations found in [Bro99a] on oxygen diffusion in ultrafine-grained undoped ZrO_2 at 500ºC. These values satisfy $\Delta = 2.2 \cdot 10^4$, whereas other ratios in the calculations were obtained by varying D_{gb} and fixing D_g. Most results shown in the present work reflect the behavior of $C_{av}(y, t)$ and the distribution of $C_g(x, y, t)$.

The main aim of the present study is to check the validity of Le Claire's relation for short-time situations and to estimate possible errors of the D_{gb} determination. An apparent GB diffusivity ($D_{gb,app}$) is introduced which can be compared with a true diffusivity $D_{gb,true}$ used in the calculation.

3.1.1 The C- or B-regime?

In order to be able to evaluate D_{gb} by using Le Claire's relation, one should only know that the condition of type-B kinetics is satisfied. The diffusion length in the bulk (grain) (L_g) was allowed to vary from a very small value of 0.77 nm at t = 2000 s. This implies an extremely short L_g of the order of atomic spacing, and high concentration gradients. Such an extreme situation corresponds to L_g which does not exceed the GB thickness (δ) significantly. One could open the question about the validity of the type-C kinetics under such conditions. In order to understand the diffusion profile calculated for condition of $L_g = 0.77$ nm corresponds more to the B-regime or C-regime, the diffusion profile was fitted by a complementary error-function with D_{gb}. If tentatively the evaluation for type-C is used, the diffusion coefficient is wrong by four orders of magnitude. It is, hence, clear that the diffusion profile does not represent a complementary error function (fig. 3.1) and, consequently, the diffusion process does not correspond to the kinetics of type-C. This also makes generally the existence of the C-regime questionable, although the situations of very small diffusion lengths are of particular interest here. According to this result, it is enough to make several jumps for the atoms moving from the GB into the grain (this is caused by the concentration gradient, what is proposed by Fisher's system (Eq. (1.6a)) to observe the B-regime.

3.2 Integrating Whipple's solution

The integration of Whipple's solution should be done very carefully, because the short t leads to steep gradients and a reduced effective region of integration. The concentrations and

penetrations are smaller. In this case both the density of integration mesh, as far as the numerical integration is concerned, and the limits of integration can be important. The constant intervals (steps) Δx or Δy, depending on the direction, determine the mesh density and are chosen to be important parameters to achieve a very well converged result. In some cases it suffices to find these steps properly. This has nothing to do with the integration step used in the quadrature formula [Pres02] since the integration was performed by using the algorithms worked out in the program MatLab [Kiu05] with applying a function 'quadl' [Mat04] based on adaptive Lobatto quadrature [Gan00]. The relevant intervals are due to the 2D nature of the problem of GB diffusion and the integral form of Whipple's solution.

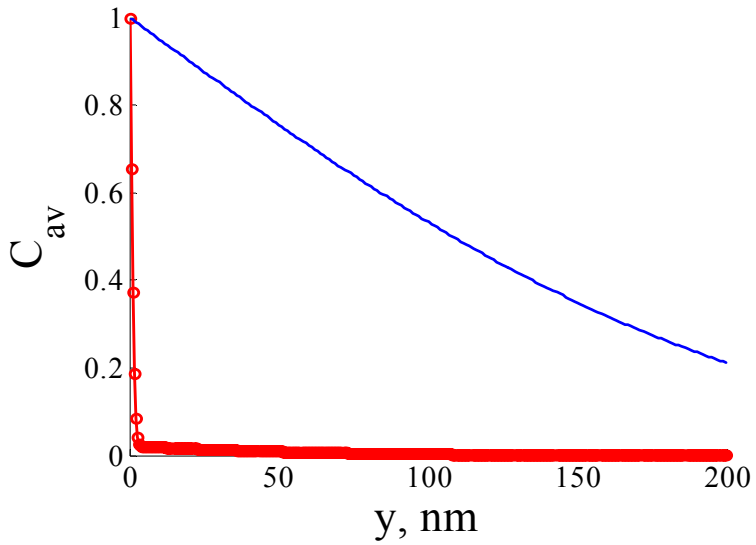

Fig. 3.1 A comparison of the Whipple (red curve) and $\mathrm{erfc}(y/2\sqrt{D_{gb}t})$ (blue curve) solutions for $\Delta = 2.2\cdot10^4$ at t = 2000 s. The concentration C_{av} is normalized with respect to C_0 (Eq. (1.3a)).

The integration was performed for each x-value along the whole length of 500 nm. Obviously, the interval Δy is of particular importance. The result is much more sensitive to this interval rather than to Δx. For this problem the convergence means that the result remains unchanged when increasing the step of integration and, at the same time, satisfying the necessary error limits. Most of the problems with the integration of Whipple's solution are related to numerical instability. Additionally, in the analysis we are interested in the derivative of the concentration profile is plotted. The derivative (in some cases the term 'gradient' is used in the present work) allows one first to analyze the physical result, and second, to estimate the quality of integration. This is reflected in the strong sensitivity of the derivative with respect to changes of the profile introduced by any numerical factors. Namely, numerical

instabilities are reflected immediately. To estimate the value of the slope of the profile (Eq. (1.16)), the scale of the ordinate ($\partial \ln C_{av}/\partial y^{6/5}$) was changed significantly due to a rapid dependence of the bulk diffusion part of the profile on y in comparison with the GB part of the profile. Thus these two parts obviously have very different rates. At each t the integration scheme (the interval Δy and the limits of integration) was verified separately for all ratios $\Delta = D_{gb}/D_g$ used, whereas the step Δx was once obtained and fixed in the calculations to 0.1 nm. The interval Δy was varied from 40 nm to 0.25 nm for $\Delta = 2.20 \cdot 10^4$ at t = 2000 s (fig. 3.2). On the one hand, the GB part of the derivative is not affected significantly when Δy is increased. This is important, because decreasing the step leads to numerical instabilities (spikes in fig. 3.2a). On the other hand, increasing the interval Δy changes the bulk part (fig. 3.2b). This is clear, because the integration of the bulk part requires smaller intervals. Interestingly, the bulk diffusion is observed up to 6 $nm^{6/5}$ at t = 2000 s for $D_g = 2.95 \cdot 10^{-4}$ nm^2/s and $D_{gb} = 6.42$ nm^2/s. At deeper penetrations only the GB diffusion plays a role. The numerical instabilities exist even with Δy = 1.0 nm, while further increasing the integration step is impossible due to deviations in the bulk part.

The integral published by Whipple [Whi54] contains Δ as the upper limit of integration and σ as the integration parameter (Eq. (1.9a)). All the curves shown in fig. 3.2 were obtained with Δ ($= 2.2 \cdot 10^4$) as the upper limit of integration (σ_{max}). In many cases Δ can be a very large value, making the region of integration too large and leading to very small concentrations. After obtaining the density of mesh (Δy = 1.0 nm), the upper limit of integration was decreased, because very low concentrations can also lead to the instabilities. Moreover, the values of concentration are so low in such regions that those do not sufficiently contribute to C_g (Eq. (1.9a)). It was observed that the numerical noise arises with σ_{max} being 15000 (hardly seen in fig. 3.3) for the same parameters that used in fig. 3.2. However, the convergence with respect to the upper limit of integration is reached with $\sigma_{max} = 20000$. Again the instabilities do not allow for a completely correct result. But, if σ_{max}, the upper limit of integration, is chosen to be small enough, the function $\partial \ln C_{av}/\partial y^{6/5} = f(y^{6/5})$ becomes even more nonlinear (fig. 3.3). In this sense, fitting the dependences $\ln C_{av} = f(y^{6/5})$ to a straight line would give very large errors in determining D_{gb}. The area under the derivative as well as its value at the maximum decreases with decreasing σ_{max}. Therefore, it is necessary to use at least $\sigma_{max} = 15000$ for the parameters $\Delta = 2.2 \cdot 10^4$ and t = 2000 s. This means one always has to find reasonable values σ_{max}, otherwise the slope can be overestimated due to numerical reasons. In fig. 3.4 the integrand of Whipple's solution is plotted as a function of σ for the same diffusion

a)

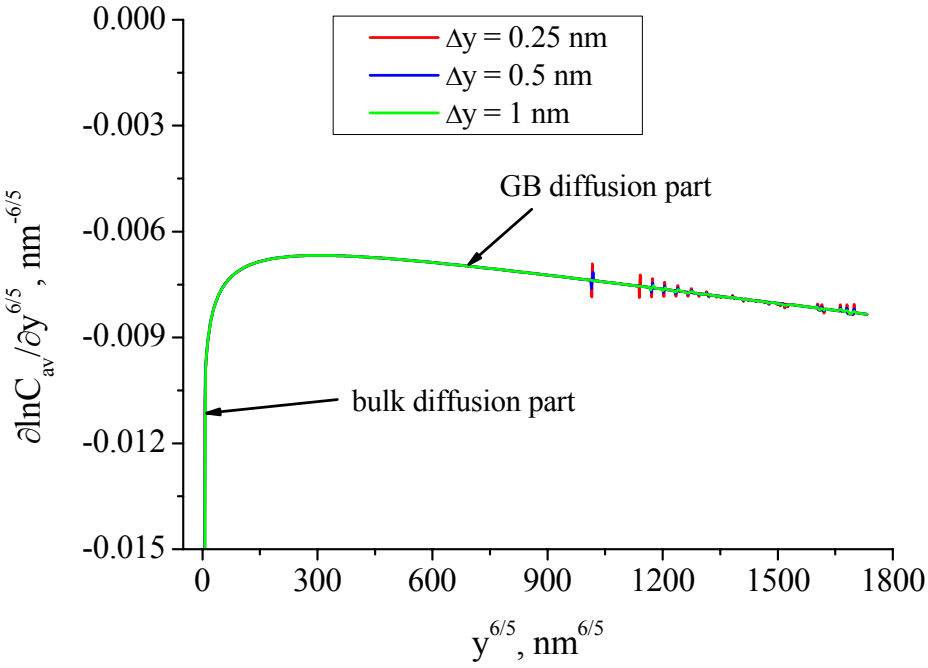

b)

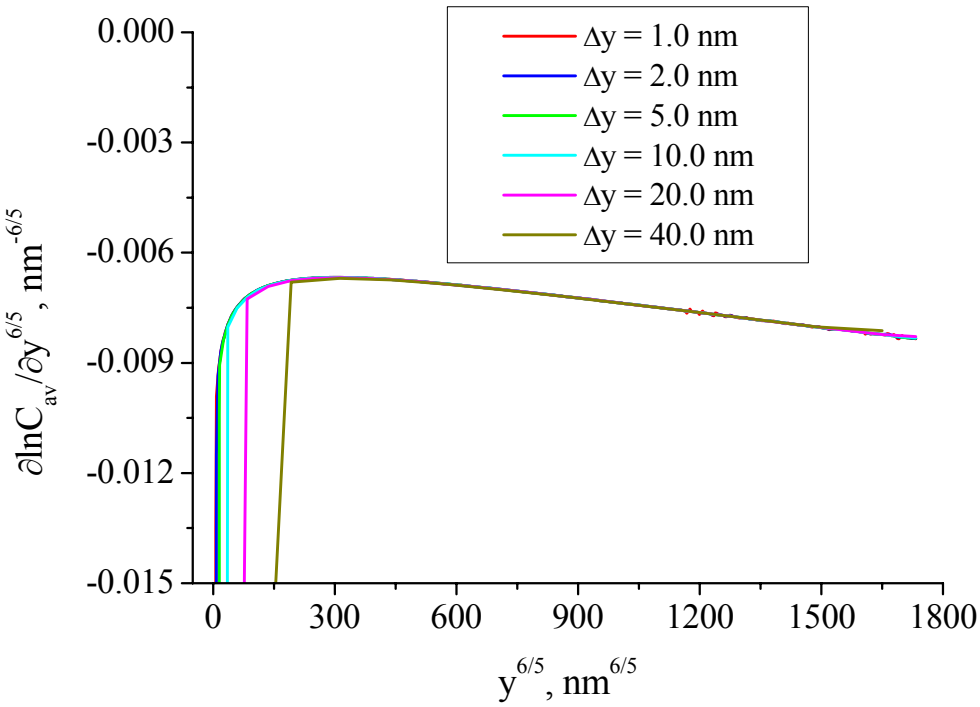

Fig. 3.2 Variation of the derivative $\partial \ln C_{av}/\partial y^{6/5}$ as a function of $y^{6/5}$ obtained for small a) and large b) Δy-steps for $\Delta = 2.2 \cdot 10^4$ and t = 2000 s.

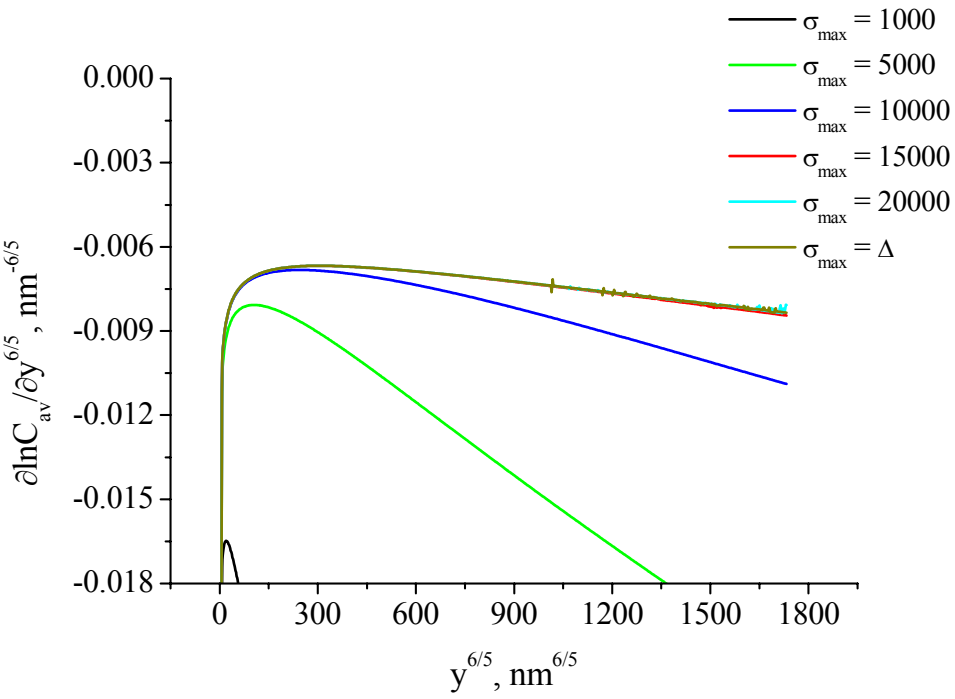

Fig. 3.3 Different upper limits of integration for $\Delta = 2.2 \cdot 10^4$ and t = 2000 s.

parameters as in figs. 3.2 and 3.3. It is clearly seen that the integrand has large values at small σ and decreases slowly with σ approaching very small values. One can conclude from this plot, that the reason of the overestimation of the slope for σ being smaller than 15000 (fig. 3.3) comes from the cut-off. In other words, the overestimation is due to lost concentrations at values of σ larger than 1000. The value of the integrand for σ = 15000 ($\Delta = 2.2 \cdot 10^4$), y = 10 nm and x = 0.25 nm, i.e. exactly at the GB since the GB thickness is 0.5 nm, is $3.77 \cdot 10^{-9}$. This is one of the highest integrand values which can be observed at these coordinates for σ = 15000. Such small values should also be taken to effectively integrate Whipple's solution. Consequently, the problem of very large Δ is especially important for integrating Whipple's solution at short t. In such cases, the diffusion length can be much shorter than the length of the sample. So shorter penetrations demand smaller integration limits. Fig. 3.4 shows the influence of increasing coordinates x and/or y. All the changes in the directions parallel with the GB or perpendicular to that lead only to a decreasing area under the integrand. The maximum of the integrand is shifted to larger and smaller σ for the increased coordinates y and x, respectively. It can be mentioned, that all the values discussed are sensitive to parameters such as diffusivities and t. An important consequence coming from fig. 3.4 is that the integral can have a maximum value at rather small y-coordinates.

Finally, different integration intervals were tried in the two parts of the diffusion profile. As it is clearly seen in fig. 3.2 the results for $\Delta y = 0.25$ nm and $\Delta y = 0.5$ nm do not deviate from each other, satisfying the error of 1%. The only problem of those is related to

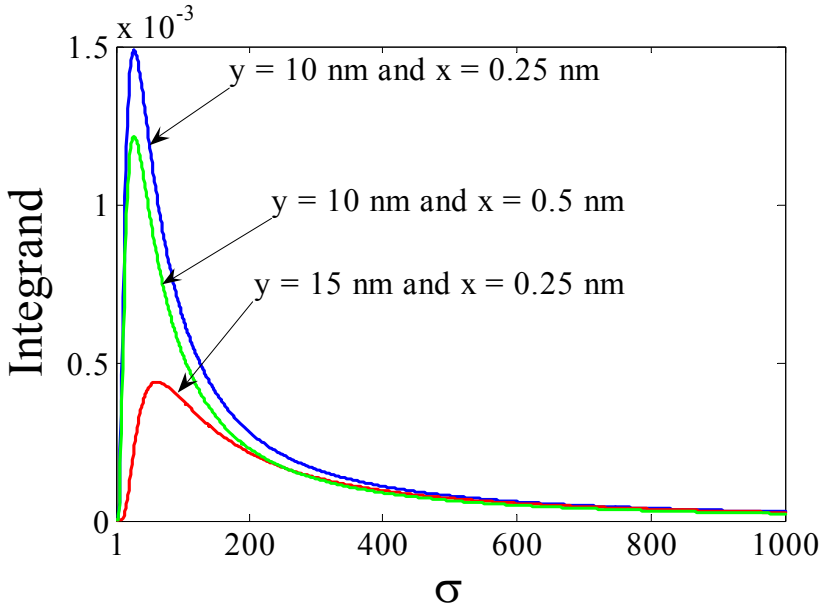

Fig. 3.4 Integrand of Whipple's solution plotted as a function of σ for different coordinates y and x.

instabilities. So $\Delta y = 0.5$ nm can be taken as integration interval in the bulk part. Because the deviations in the GB part arise with Δy being larger than 10 nm, that value is suggested to be a limit of integration in the GB part. In fig. 3.5a the results of integration with different intervals in the two parts of the profile are compared with the result obtained with a constant step. The bulk part was integrated up to a penetration of 50 nm, which exceeds the bulk diffusion length and lies in the region of obvious intermixing between the bulk and GB parts of diffusion. The result of integration with two intervals is in a very good agreement with the result of constant integration interval. Consequently, different integration intervals should be used at t = 2000 s in order to exclude any numerical problems and to obtain accurate results.

The increase of t allows the same interval of integration to be used for both parts of the derivative. Thus, the numerical instabilities disappear already at t = 4700 s with $\Delta y = 1$ nm due to an increased level of concentration in both the bulk and GB parts of diffusion profile (the length of the sample is fixed). Nevertheless, the deviations in the bulk part with increasing Δy seem to be similar to those observed at t = 2000 s up to 13200 s despite the fact

a)

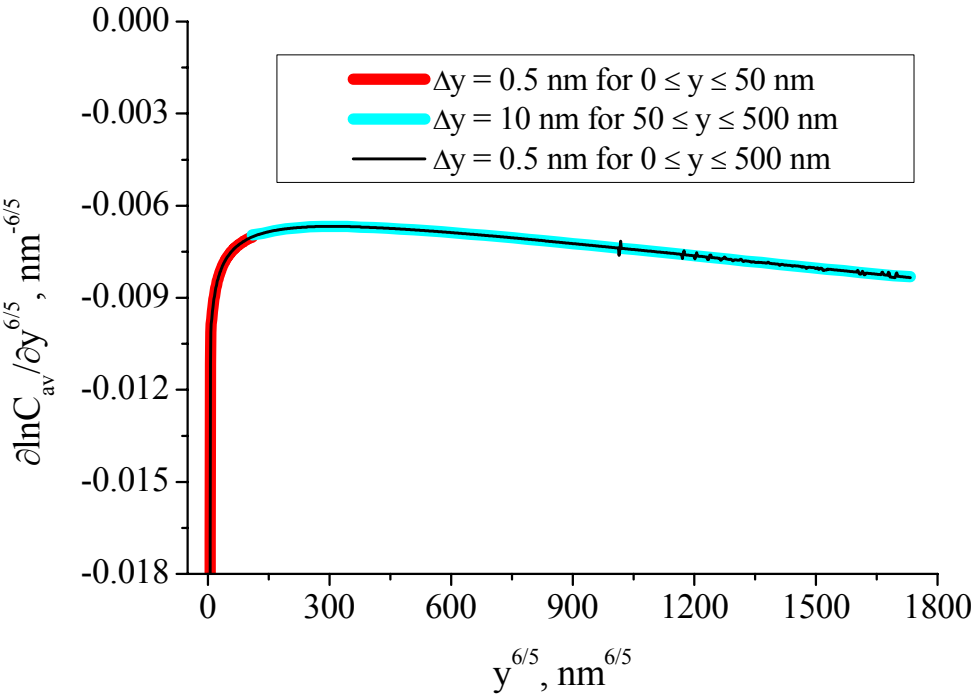

b)

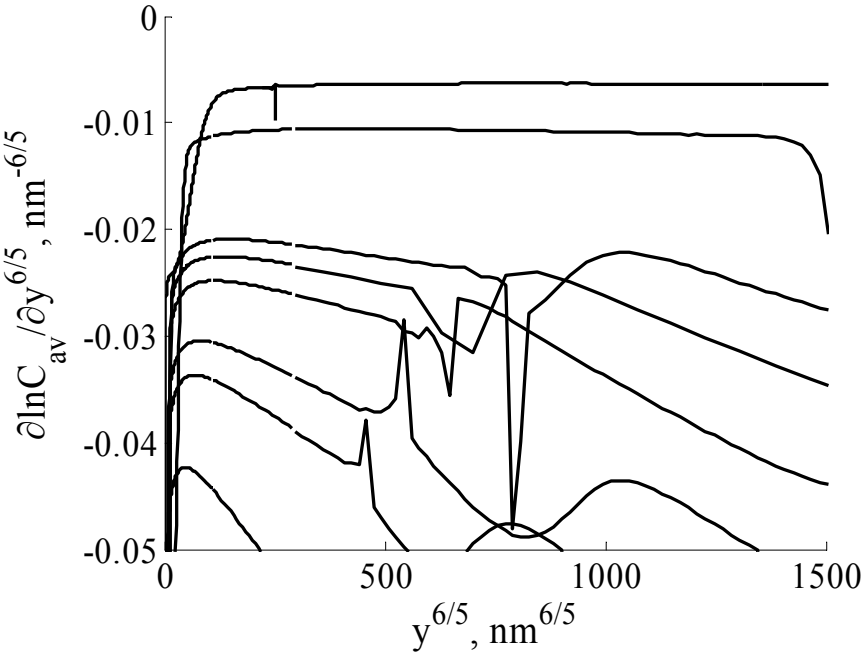

Fig. 3.5 a) A comparison of different integration schemes at t = 2000 s and $\Delta = 2.2 \cdot 10^4$, b) An example of the numerical instabilities for $\Delta = 10^3$ at different t (note: the slope decreases with t).

that the derivative of the bulk part changes with t too. Finally, the step in the bulk part was successfully varied in the calculations from 0.5 nm at t = 2000 s to 5.0 nm at t = 500000 s.

Such a situation is remaining until the interval becomes too small for the integration of the GB part. One can observe similar instabilities as shown in fig. 3.5 for t = 13200 s: the problem of low concentrations is replaced by another one, the small changes of the derivative in the GB diffusion part. In this case the variation of σ_{max} cannot longer improve the result and only integrating with different intervals in different parts of the profile allows again a qualitative result to be obtained. An example of the instabilities arising in the integration is also presented in fig. 3.5b.

3.3 Errors in determining the grain boundary diffusivity

As far as the procedure of integrating the Whipple solution is clear, one can examine different t and Δ. As it was explained above, the length and the width of the sample (geometrical model) were fixed to 500 nm and 25 nm, respectively. This exactly reflects the isolated boundary arrangement (fig. 1.2). Recently, many theoretical works on the evaluation of Whipple's solution were published which are based on the transformation of the solution directly to the average concentration $C_{av}(y, t)$ [Chu96b], [Eva97], [Sha98]. Such transformations are not used here but will be discussed in the following sections. Also, the integration used in the present work is very similar to what is done experimentally.

The result obtained by simply integrating Whipple's solution is depicted in the following figure for $\Delta = 2.2 \cdot 10^4$ at t = 2000 s:

a)

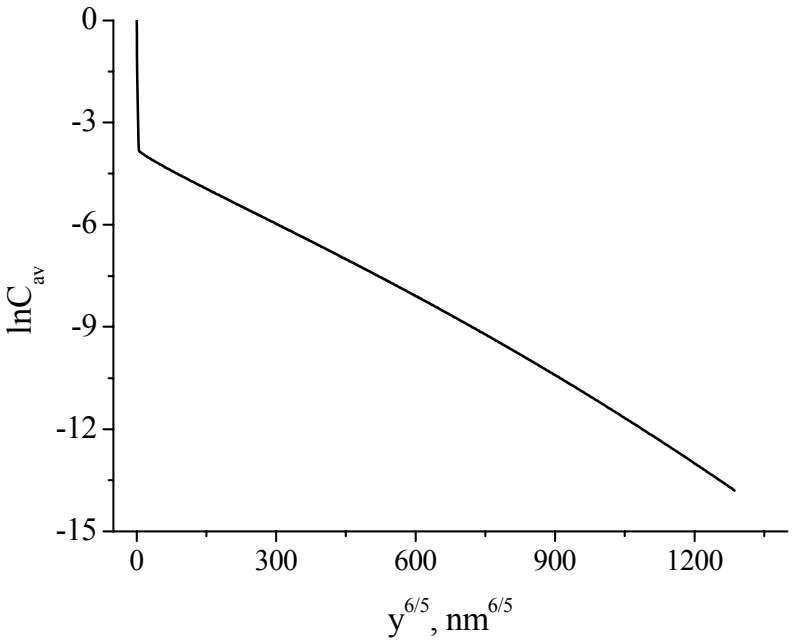

b)

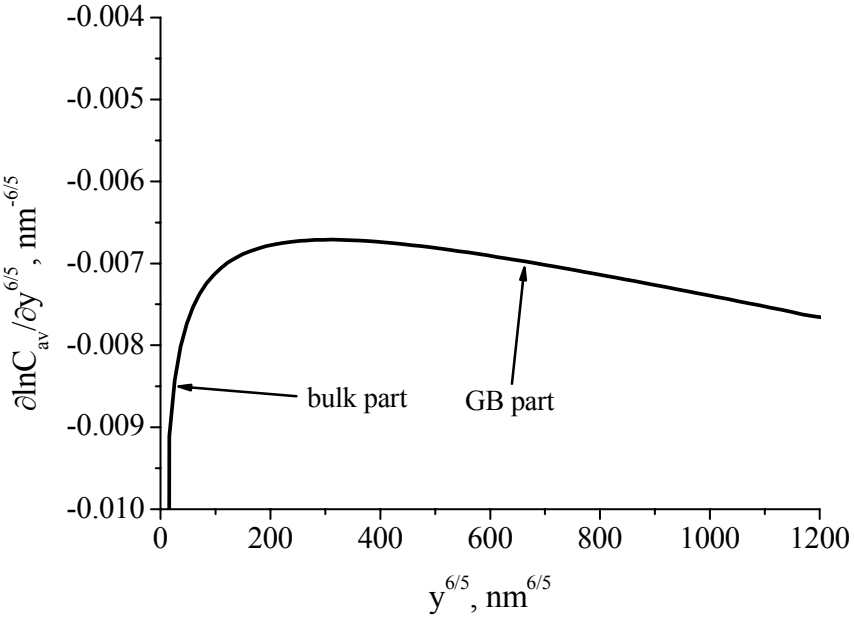

Fig. 3.6 Variation of $\ln C_{av}$ a) and $\partial \ln C_{av}/\partial y^{6/5}$ b) with $y^{6/5}$ calculated for $\Delta = 2.2 \cdot 10^4$ ant t = 2000 s.

In fig. 3.6a one can see a typical diffusion profile, comprising two distinguishable parts: a near surface part (or so-called bulk part) and a deeper penetration tail due to the GB diffusion. As it was mentioned above, the slope of the GB part gives D_{gb} according to Le Claire's relation (Eq. (1.16)). There are two possibilities to verify such a slope. One of them is to fit the GB part of profile by a straight line subtracting the bulk part. This is usually done in the experiments [Her05], [Yas97], [Kow00], [Bak02]. However, the profile is expected to be a nonlinear function of $y^{6/5}$, and the nonlinearity of its GB part can strongly depend on the depth. Consequently, another possibility might be preferred, namely to plot the derivative of the profile in order to estimate the effect of nonlinearity. Fig. 3.6b shows that indeed the profile is nonlinear, i.e. the derivative simply confirms this.

At some point ($y^{6/5} \sim 300$ nm$^{6/5}$ in fig. 3.6b) the derivative is characterized by a maximum which is close to the bulk part but, in fact, corresponds to the GB part. In the present study it is proved, that this maximum gives the correct slope or, at least, the smallest error to find D_{gb} using Le Claire's relation. To prove this statement, the diffusion profiles were calculated by using Whipple's solution at different t, varying Δ from 10^2 to 10^5.

According to fig. 1.5 (the diffusion lengths dependences with t), calculating the profiles up to t = 500000 s guarantees the B-regime for different ratios Δ. The slope of the profiles decreases with t, and this is clearly seen in the dependences $\ln C_{av} = f(y^{6/5})$ (fig. 3.7a). The same behavior, obviously, can be observed for all other ratios Δ (fig. 3.8). Importantly, the slope varies with t striving for some saturation at the maximum (figs. 3.7b and 3.8). However, this saturation can never be reached. It means only that having an opportunity to obtain the profiles at very long t, as it is the case for coarse-grained materials; one can observe the values of D_{gb} rather independent of the effects of the GB diffusion nonlinearity. This might be the reason why the effect of nonlinearity has not yet been discussed in the literature. However, the effect of nonlinearity is more pronounced at shorter t. Therefore, the derivative varies with t and along the coordinate y (fig. 3.7b and fig. 3.8). Importantly, all the profiles and their derivatives, shown in figs. 3.7b and 3.8, were calculated for one maximum value of the depth (the length of geometrical model) for Δ being $2.2 \cdot 10^4$ and 10^5, namely 500 nm. For $\Delta = 10^2$ the maximum depth was 40 nm at t = 2000 s and 500 nm at $t \geq 100000$ s in order to exclude the effect of very small concentrations. This is done because C_{av} at y = 40 nm for $\Delta = 10^2$ and y = 500 nm for larger Δ at t = 2000 s is about $0.3 \cdot 10^{-6}$. One may conclude that deeper penetrations than those used in figs. 3.7 and 3.8, can lead to larger errors in determining D_{gb} [Gry05].

The calculated profiles were fitted by a straight line according to the procedure usually used in the experiments and relevant errors in determining D_{gb} were obtained (fig. 3.9, black lines). The error and derivative vary with t. This is reflected in the decreasing error. At longer t the slope is more correct than at shorter ones (again the length of the sample was fixed). It does not mean that the error cannot be larger at long t. The value of the error is only a matter of the nonlinearity of profile. This increases, if deeper diffusion profiles are used. Interestingly, the fitting gives slopes which more strongly deviate from those at the maximum as t shortens. The same can be observed in the case of smaller ratios Δ. The profile is even more nonlinear under conditions of small Δ, giving larger errors. The error is about 45% at 2000 s for $\Delta = 10^2$.

The derivatives plotted in fig. 3.8 demonstrate that the slope is larger at shorter t, decreasing the apparent D_{gb} ($D_{gb,app}$) when applying the Le Claire relation. That is why D_{gb} is underestimated when the diffusion profile is fitted by a straight line, especially in the cases of short t and, as a consequence, short diffusion lengths. The maxima of derivatives of calculated profiles were also put into Le Claire's relation. Taking the values of the derivatives at the maximum allows one to reduce the error (fig. 3.9, red curves). It can be understood in such a way, that the diffusion process developing around and along a GB passes through different conditions, and there is only one situation corresponding to the considered diffusion regime. The deeper the penetration depth the smaller the contribution of GB to diffusion in the grain and the lower the level of concentration around and within the GB. Therefore, the whole process is becoming to be concentrated within the GB. In other words, the contribution of GB is not simply a linear process of $y^{6/5}$ or any other power law.

Interestingly, the error for $\Delta = 2.2 \cdot 10^4$ and 10^5 (fig. 3.9b) increases at longer t. In these cases the maximum was not reached for the used length of the sample (for example, the curve for t = 500000 s in fig. 3.8c), although the diffusion profile itself still comprises the two distinguishable parts. This opens a question about an additional effect related to the nonlinearity. One may conclude that the length of the whole geometrical model may be too great giving the slope affected by the new conditions along the depth or too short giving the slope affected by the bulk part of the diffusion profile [Kau95]. In both cases the concentrations and derivatives are smaller than those at the maximum. In these cases the derivative does clearly show how the profile is affected. The discussion of short lengths of the sample will be continued in the next section.

a)

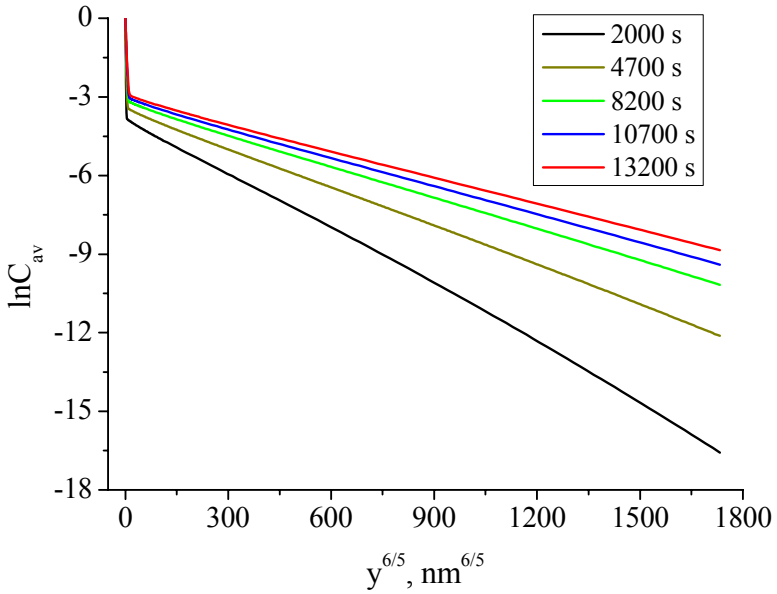

b)

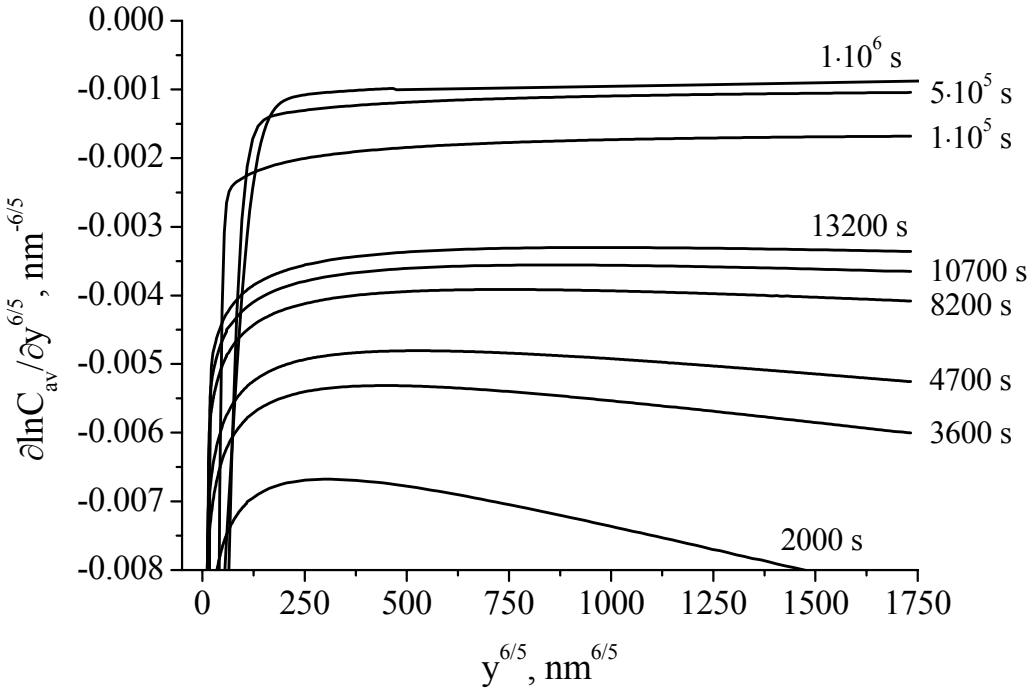

Fig. 3.7 Variation of $\ln C_{av}$ for t = 2000 s – 13200 s a) and $\partial \ln C_{av}/\partial y^{6/5}$ for t = 2000 s – $1 \cdot 10^6$ s b) with $y^{6/5}$ calculated for $\Delta = 2.2 \cdot 10^4$.

When the positions of the maxima are known, one would compare them with a criterion, which has already been discussed in the literature [Moy91], but very often ignored in the evaluation of experiments. The criterion is based on the relationship between y and L_g. According to this criterion, the determination of D_{gb} should be done from those parts of measured diffusion profile, which satisfy $y \geq 5L_g$. In the calculations L_g is the same for all ratios Δ used and depends only on t, because D_g was fixed. However, the ratio Δ increases, and the position of maximum goes from $y_{max}^{6/5} \sim 12$ nm$^{6/5}$ for $\Delta = 10^2$ at t = 2000 s (the corresponding diffusion length $L_g \sim 0.77$ nm) to $y_{max}^{6/5} \sim 1732$ nm$^{6/5}$ for $\Delta = 10^5$ at t = 500000 s (which is, in fact, not the position of maximum, but simply corresponds to the depth of 500 nm, $L_g \sim 12$ nm). The positions satisfy the criterion by being 10 times larger than L_g for $\Delta = 10^2$ at t = 2000 s and 42 times larger than L_g for $\Delta = 10^5$ at t = 500000 s. So the criterion is very rough. It only reminds one that the GB part of diffusion profile is influenced by the bulk diffusion part. The criterion is still not absolutely correct and even misleading when the profile is fitted by the straight line.

It is interesting to analyze here how the maximum appears. In fig. 3.10 solutions given by pure bulk diffusion (a complementary error-function in the case of a constant source) and by Whipple's solution excluding bulk diffusion (pure GB contribution) are presented separately for $\Delta = 10^5$ at t = 500000 s and t = 2000 s. A sum of both contributions gives C_{av} obtained by integrating Eq. (1.9a), also shown in fig. 3.10. The bulk diffusion solution decreases rapidly in comparison with the GB diffusion part. Whipple's solution coincides with purely bulk diffusion at very small coordinates and then is influenced by both contributions, and for larger y-coordinates dominates by the GB part. The GB contribution becomes predominant at around 110 nm$^{6/5}$ in fig. 3.10a, what is much smaller (by a factor of 16 in this nonlinear scale) than the position of the corresponding maximum ($y_{max}^{6/5} \sim 1732$ nm$^{6/5}$). Normally, for the parameters involved one needs a length of the sample larger than 500 nm in order to reach the maximum at long t. The maximum can correspond to the beginning of the B-regime since the diffusion regimes change each other not only with time but also along y [Kau95]. This regime finishes when the derivative goes down. The position of the maximum for $\Delta = 10^5$ at t = 2000 s (fig. 3.10b) is about 763 nm$^{6/5}$, what is 100 times larger (on the nonlinear scale) than the coordinate at which the GB part becomes the solution determining part. The longer t obtains a much more slowly varying function, suggesting the slope to be very small, whereas shorter t gives higher derivatives. In both the cases the overall solution is determined by the bulk diffusion part only at extremely small depths, i.e. of the order of several nanometers.

a)

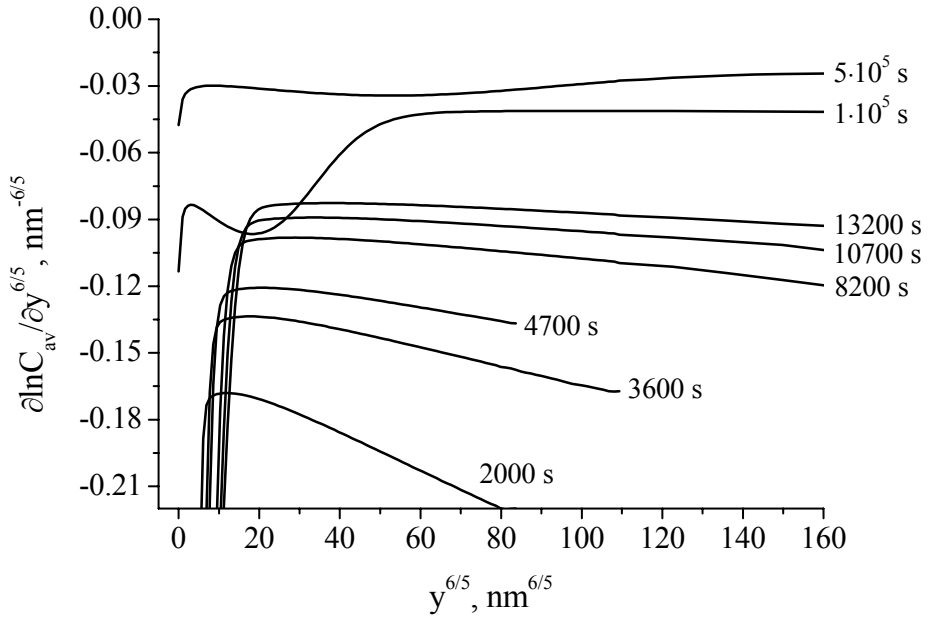
0.00
-0.03
-0.06
-0.09
-0.12
-0.15
-0.18
-0.21
0
20
40
60
80
100
120
140
160
$\partial \ln C_{av}/\partial y^{6/5}$, nm$^{-6/5}$
$y^{6/5}$, nm$^{6/5}$
5·10^5 s
1·10^5 s
13200 s
10700 s
8200 s
4700 s
3600 s
2000 s

b)

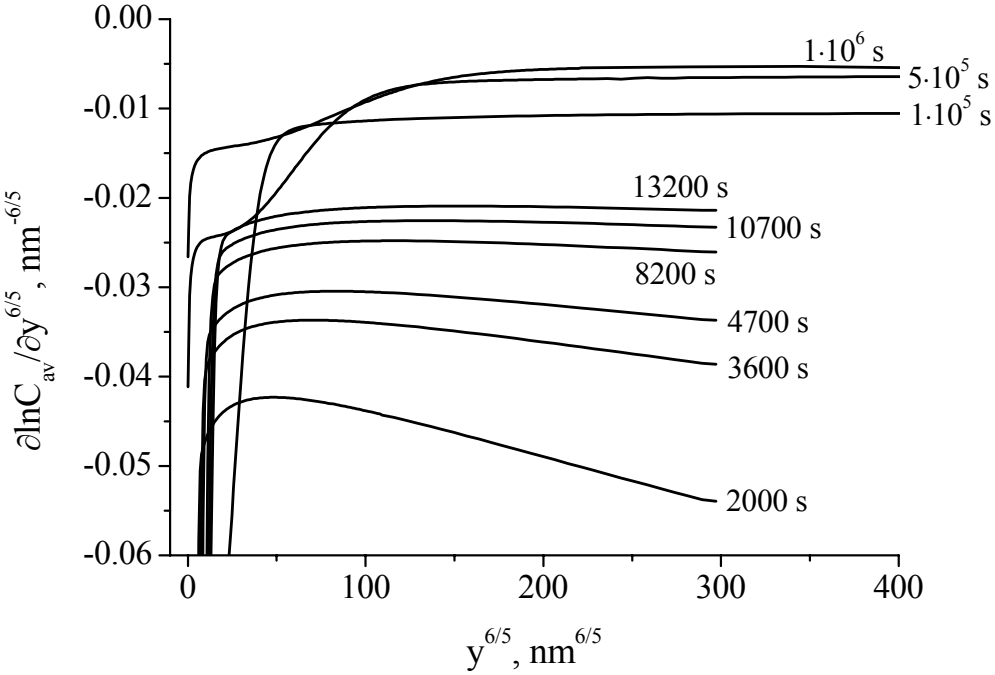
0.00
-0.01
-0.02
-0.03
-0.04
-0.05
-0.06
0
100
200
300
400
$\partial \ln C_{av}/\partial y^{6/5}$, nm$^{-6/5}$
$y^{6/5}$, nm$^{6/5}$
1·10^6 s
5·10^5 s
1·10^5 s
13200 s
10700 s
8200 s
4700 s
3600 s
2000 s

c)

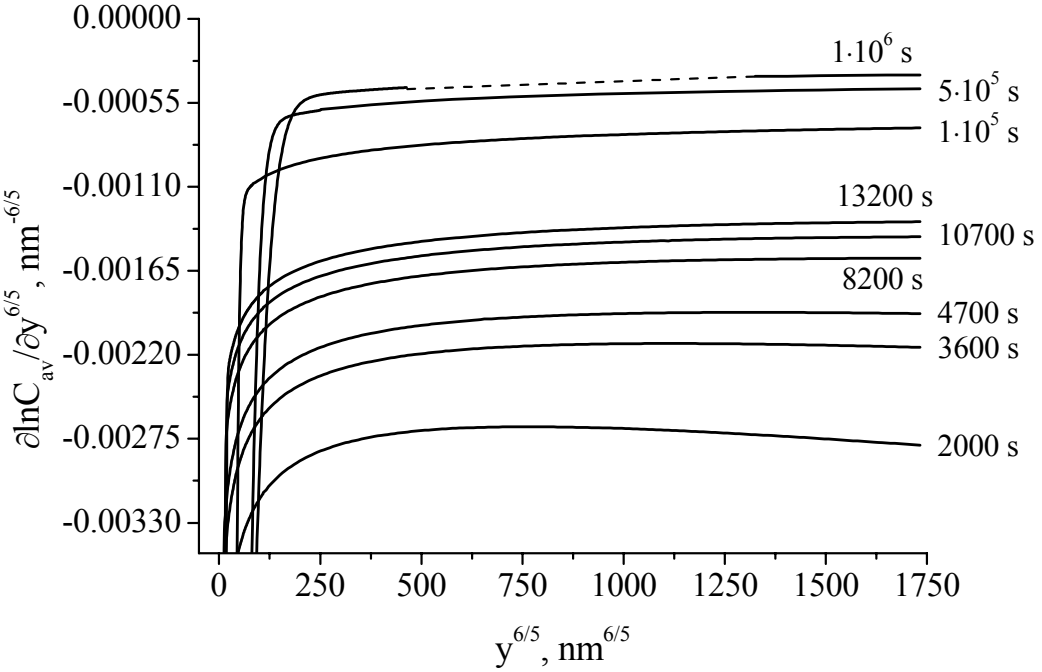

Fig. 3.8 Variation of the derivative $\partial \ln C_{av}/\partial y^{6/5}$ with $y^{6/5}$ obtained for a) $\Delta = 10^2$, b) $\Delta = 10^3$, c) $\Delta = 10^5$. The dashed line means that the integration in this region was very unstable and, therefore, impossible.

3.3.1 Nonlinearity and small values of dimensionless parameter w

The parameter w (Eq. (1.15)) is a very helpful quantity as regards understanding the conditions of the developing diffusion process. The problem of this parameter is in fact that its knowledge requires the knowledge of the diffusion coefficient D_{gb}. Meanwhile, the parameter makes the diffusion profiles plotted as a function of w for fixed t independent of the ratio of diffusivities Δ. This seems to be one of the main reasons, why Le Claire suggested the derivative $\partial \ln C_{av}/\partial w^{6/5}$ to be constant [Cla63]. Moreover, Le Claire mentioned that w should be larger than 2 to use his relation. On the other hand, the condition of $w << 2$ can be understood, if the gradient $\partial \ln C_{av}/\partial y^{6/5}$ is analyzed. As it was mentioned above, the contribution of bulk diffusion to the concentration profile is very restricted, because of interference of bulk diffusion with GB diffusion. The interference starts at surprisingly small values of y. The reason is that the derivative changes its value going slowly through the maximum and then decreasing due to the GB contribution only. In fig. 3.11 the dependence of

a)

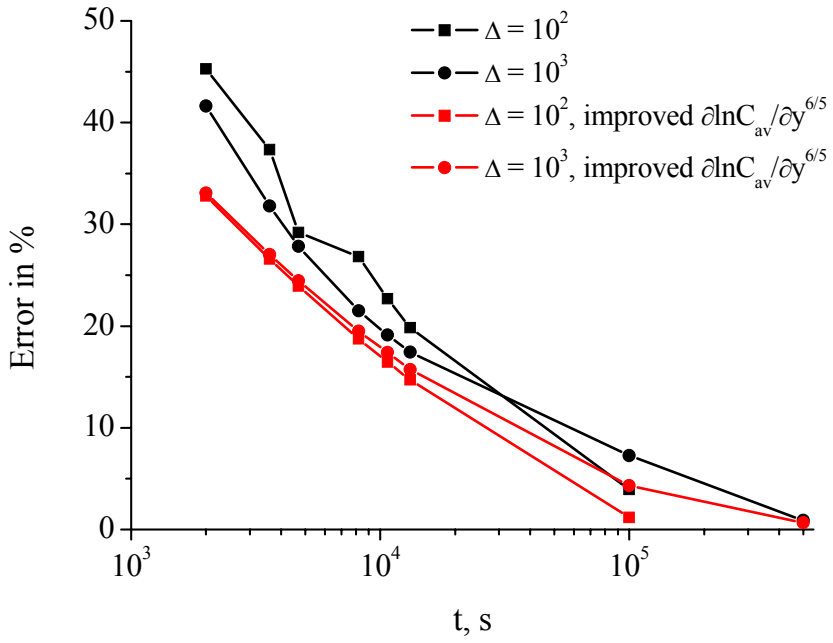

b)

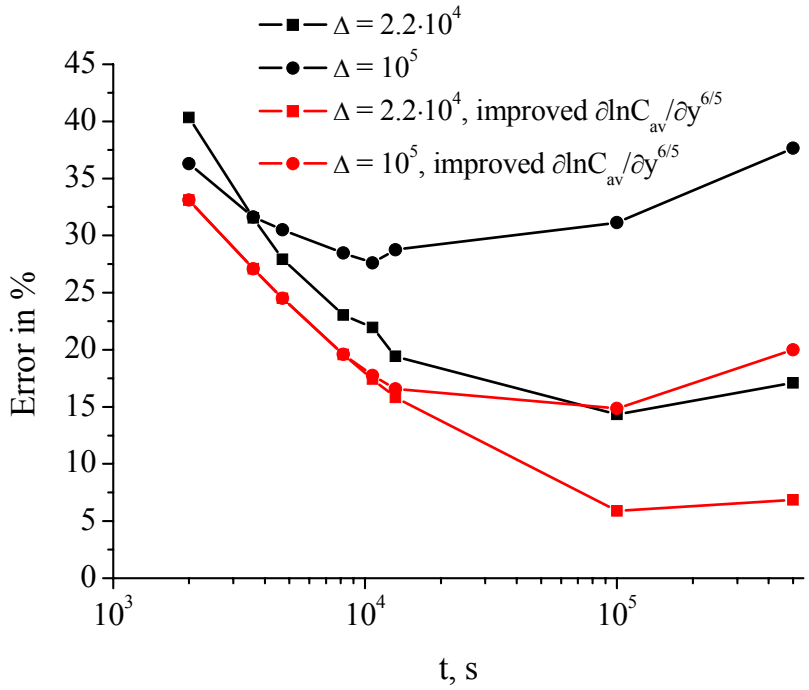

Fig. 3.9 Variation of the errors in determining D_{gb} with time ($D_{gb,app}$ was obtained by using Le Claire's relation): a) $\Delta = 10^2$, $\Delta = 10^3$, b) $\Delta = 2.2 \cdot 10^4$, $\Delta = 10^5$. Errors were estimated according to $\left(\left|D_{gb,app} - D_{gb,true}\right| / D_{gb,true}\right) \cdot 100\%$.

a)

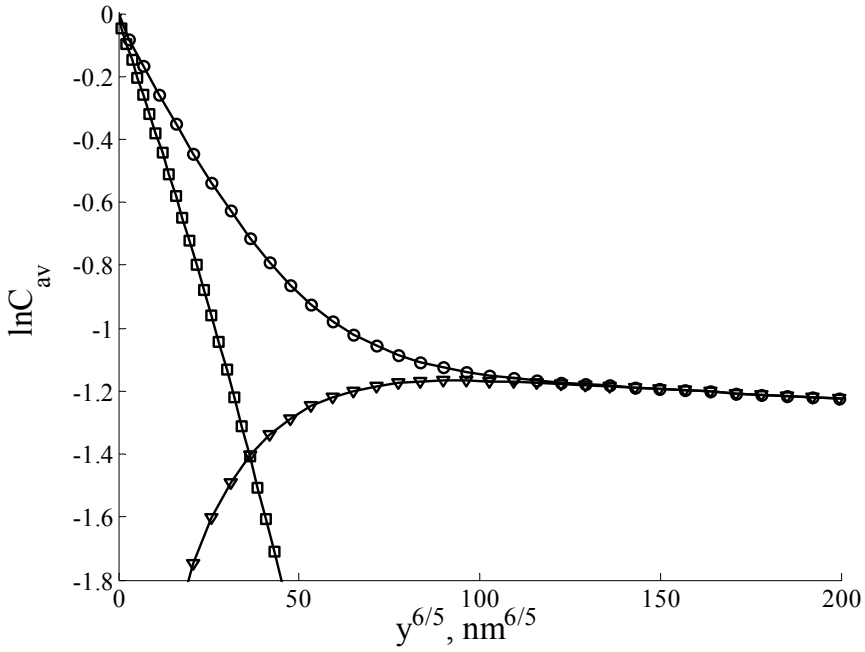

b)

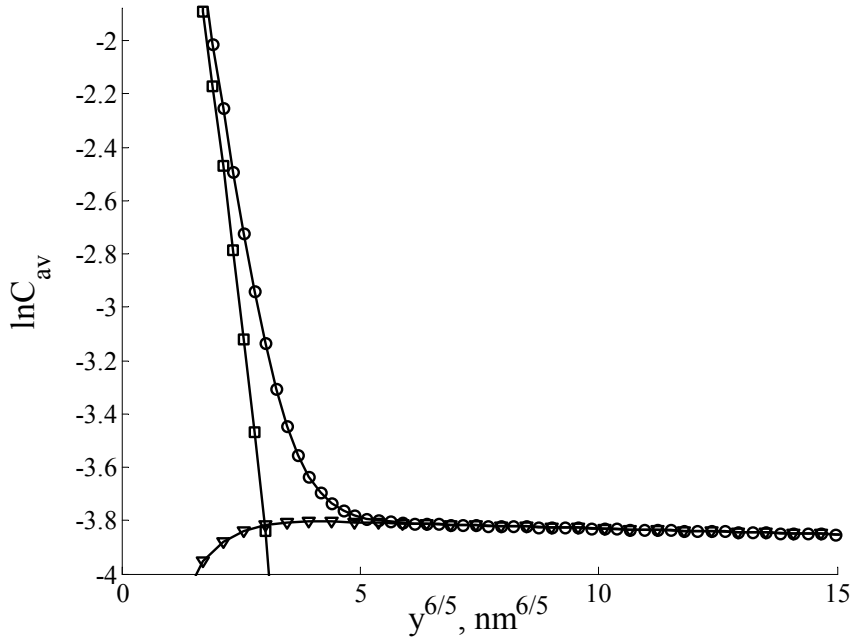

Fig. 3.10 Whipple's solution (circles) compared with its bulk part (squares) and GB part (triangles) at t = 500000 s a) and 2000 s b) for $\Delta = 10^5$.

the dimensionless parameter w on the real coordinate y is shown for different t, where the domain of inapplicability of Le Claire's relation is determined by values of w less than 2. Despite the fact of very different t, 2000 s and 500000 s, the values of w can be either smaller or larger than 2. In the dominator of w is the square root of $D_g t\beta$. While the β - parameter (Eq. (1.9d)) decreases with the diffusion time as $t^{-1/2}$, the positional coordinate y can be increased – both facts lead to the compensated values of w. The value of 2 is reached at smaller y, if t is decreased, because the shown linear dependences have different slopes. This looks like that there is a higher probability to arrive to the conditions of $w << 2$ for longer t, because the range of y is larger than for shorter t. One should keep in mind that the increase of t is only possible for a polycrystalline sample having larger grains, and deeper penetrations are needed to observe the nonlinearity. Particularly, at higher t the position of maximum is shifted to larger values of y. Correspondingly, the values of w larger than 2 for t = 500000 s arise at sufficiently larger values of y in comparison with t = 2000 s. An interesting question to be addressed is about the shape of diffusion profile at different w.

In order to analyze the diffusion profiles for different values of w, y was varied from 0 to 500 nm for t = 2000 s and $\Delta = 2.2 \cdot 10^4$. It is clear, that small values of w correspond to those parts of the diffusion profile, which are mostly influenced by bulk diffusion (fig. 3.12a). If the dimensionless parameter (w) increases, the profile changes from steep part to the interference part. Such a behavior continues until the maximum of the derivative is reached as it was observed for the dependences on the real coordinate. The corresponding diffusion profiles were plotted for considered w-values (fig. 3.12b). Surprisingly, the shape of those profiles in the dependence $\ln C_{av} = f(y^{6/5})$ represents classical, usually expected, diffusion profiles, comprising two distinguishable parts due to bulk diffusion and GB diffusion separately. Consequently, D_{gb} can be found from such dependence by applying Le Claire's relation. However, this would cause errors since the maximum is not reached. Thus the qualitative estimation of the profile leads to the situation when D_{gb} is found according to the procedure, which is not straightforward. This also allows the problems discussed in [Chu96a] to be better understood. In the latter paper, errors of the order of 70% were observed. However, an explanation of those errors was not given. Instead, they suggested a new expression for the δD_{gb}-product which requires the knowledge of new fitting parameters summarized in this paper. According to the present analysis, the maximum of the gradient gives an accurate result and many problems of using the conventional procedures are related to the nonlinearity.

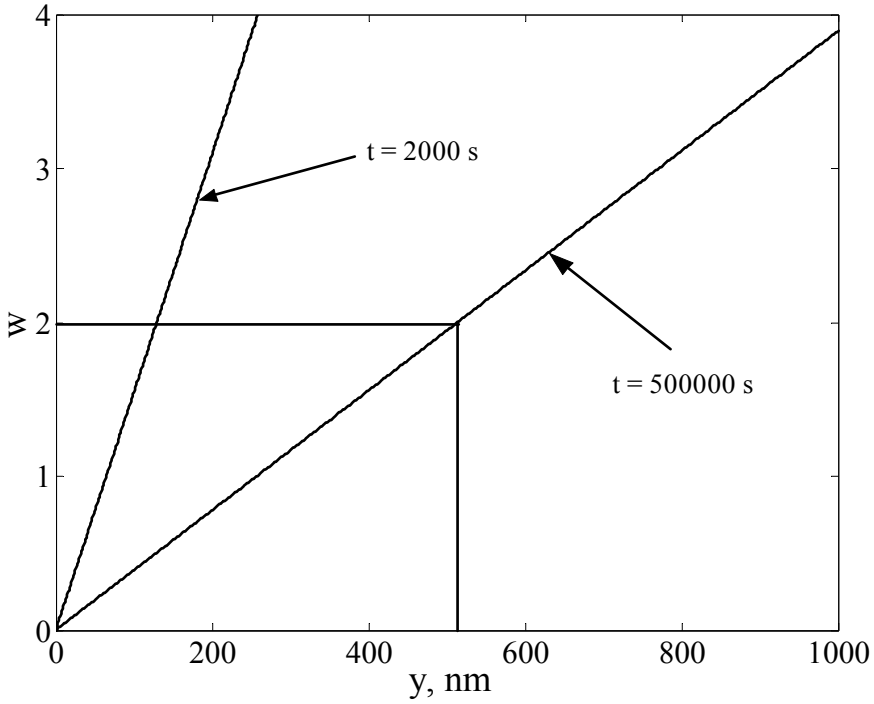

Fig. 3.11 Dependence of the dimensionless quantity w on real positional coordinate y for t = 2000 s and t = 500000 s.

3.3.2 Analyzing the errors of using Le Claire's constant

In fig. 3.9 the errors of finding the GB diffusivity (D_{gb}) remained high, even after using the maximum of the derivative. It was supposed that an additional problem is related to Le Claire's constant ($\partial \ln C_{av} / \partial w^{6/5} \approx -0.78$, Eq. (1.14)) as being the only quantity, which was not discussed up to now. As far as the diffusion profiles were obtained for different ratios Δ and t, the derivatives of those as functions of dimensionless coordinate w were also plotted. The deviations of the derivative from Le Claire's constant were observed and estimated. In fig. 3.13 the derivatives are depicted for the same ratios Δ and t as in fig. 3.8. The qualitative picture is similar, but the meaning is different. Interestingly, the derivatives for different Δ have the positions of maxima at the same w which vary from 2 to 6, depending on t. For the smallest ratio $\Delta = 10^2$ Le Claire's constant is reached at t = 100000 s due to β close to 1 in contrast to other ratios. This is an exception case which refers to small Δ which is unlikely in diffusion experiments, unless small angle grain boundaries are concerned. Thus, for the ratios Δ larger than 10^2 it takes at least 500000 s to reach Le Claire's constant for the diffusion parameters used in the present study. An important property of the dependences in figs. 3.13c and 3.13d is in fact that these become more and more restricted with t. Comparing the dependences for $\Delta = 2.2 \cdot 10^4$ and $\Delta = 10^5$ demonstrates that the values of w are twice as large

as in the former case, while the positions of maxima are approximately the same. This is related to the values of β and the length of the sample remaining constant. Large values of w always mean very deep profiles characterized by nonlinearity, what was also considered in the theoretical study of Le Claire [Cla63]. The nonlinearity in his profiles is obvious, but Le Claire did not discuss this property properly. Therefore, the tendency is that the position of maximum shifts to higher values of w, and that the maximum value of derivative tends to Le Claire's constant as t grows. Both facts make the dependence more and more parallel to the abscissa, i.e. tending to a constant value for a fixed length of the sample. In this sense one may expect that there can be situations depending on the parameters in which the derivative is, to some extent, a constant value. Consequently, high temperatures and/or long diffusion times lead more or less to Le Claire's constant.

The Le Claire constant is reached for very different values of β, varying from 2 for $\Delta = 10^2$ at t = 100000 s to 2000 for $\Delta = 10^5$ at t = 500000 s. These values cover a wide β-range in comparison with Le Claire's work. Consequently, the values of β do not really determine the accuracy of the result. However, y and t are relevant for the deviations from Le Claire's constant. It is very likely that diffusion in ultrafine-grained materials (or nanocrystalline materials) is studied under conditions of short t and penetrations. That is why the measured diffusion profile can be obtained for $w << 2$. This effect has already been observed by Chung [Chu96a] when measuring the diffusion profile for MgO bicrystal. The latter point is discussed below. Importantly, the maxima of the derivatives correspond only to values of w larger than 2 according to fig. 3.13.

As the maxima of the derivatives on the real coordinate are known from fig. 3.8, then one may estimate the maxima of derivatives on the dimensionless coordinate and put both into the original expression of Le Claire (Eq. (1.14)). Following this procedure, the evaluation of errors for finding D_{gb} was continued (fig. 3.14). The errors are greatly reduced at shorter times, namely from 35% to very small errors not exceeding 1%. Nevertheless, the errors for larger ratios Δ and longer t are still high and increase with t. The reason comes from the $\partial \ln C_{av}/\partial w^{6/5}$ values taken at the maximum, while the length of geometrical model (500 nm) gives shorter values of w. These values were taken at the maxima to be in accordance with procedure used for shorter t. The dashed curves in figs. 3.13c and 3.13d show how the length was increased to reach the maximum for longer t. However, these values obviously give larger errors. By using the values found at the depth of 500 nm being the length of geometrical model, the error was decreased (red and blue points in fig. 3.14).

a)

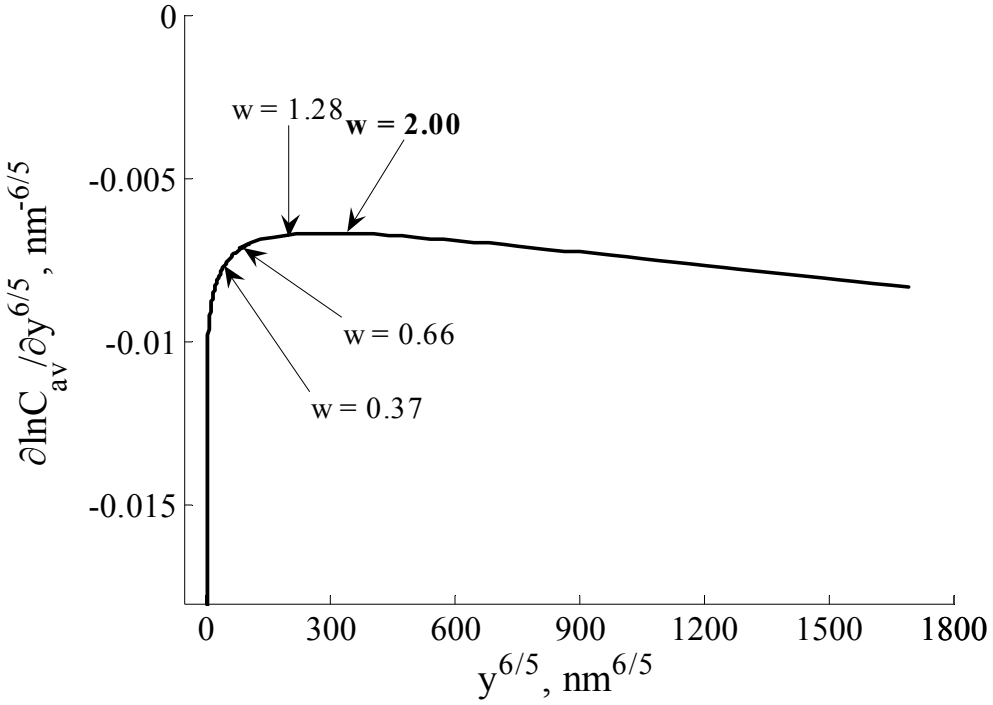

b)

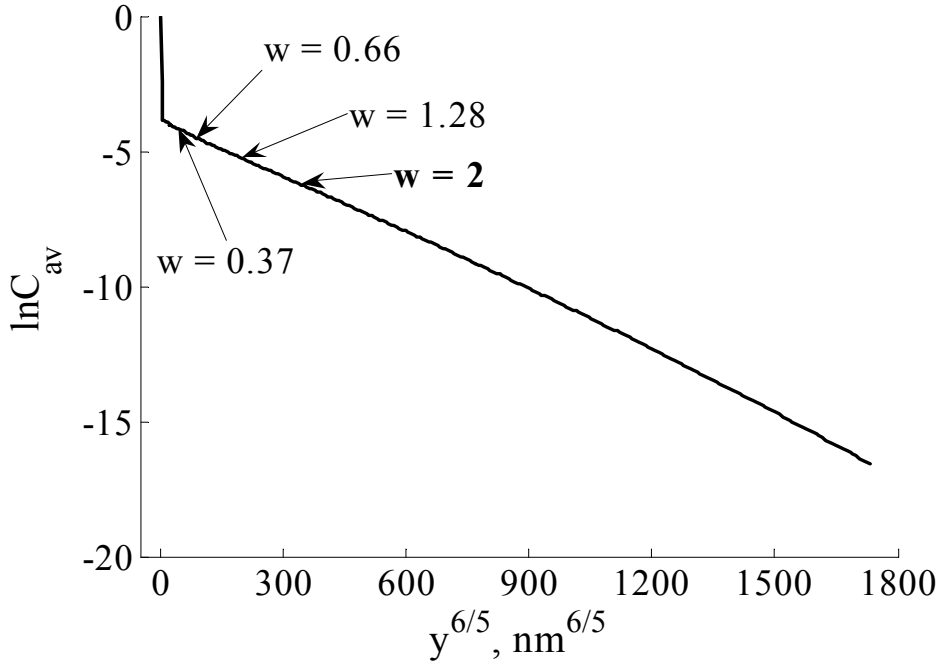

Fig. 3.12 Variation of the dimensionless quantity w as a function $y^{6/5}$ along the derivative of the diffusion profile a) and the diffusion profile b) calculated for $\Delta = 2.2 \cdot 10^4$ at t = 2000 s.

a)

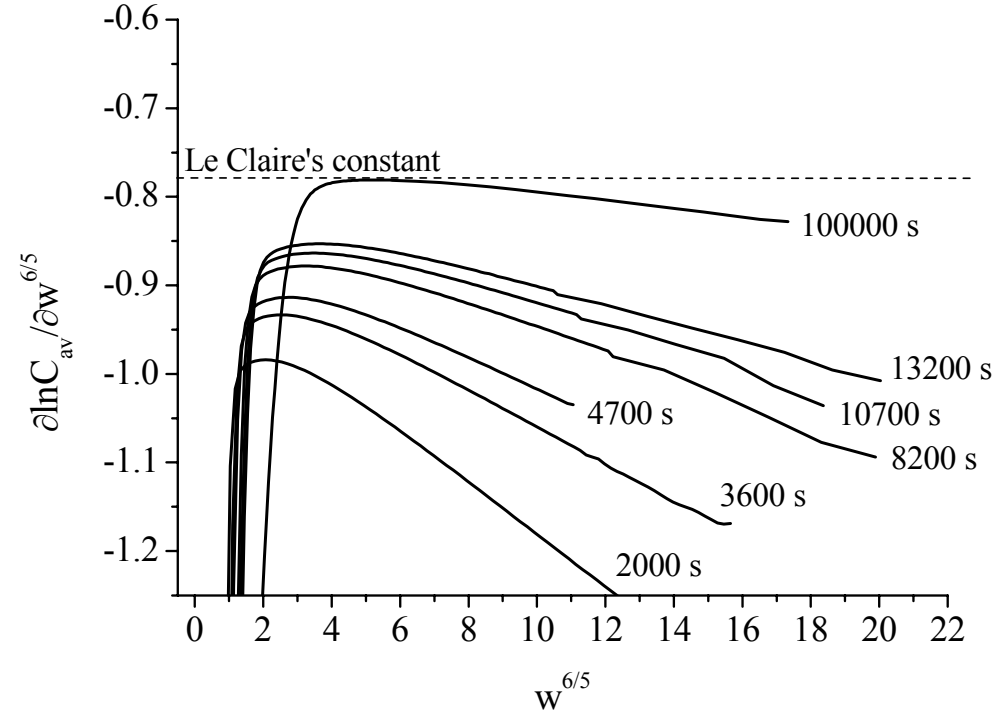
-0.6
-0.7
-0.8
-0.9
-1.0
-1.1
-1.2
Le Claire's constant
100000 s
13200 s
10700 s
8200 s
4700 s
3600 s
2000 s
0
2
4
6
8
10
12
14
16
18
20
22
$\partial \ln C_{av} / \partial w^{6/5}$
$w^{6/5}$

b)

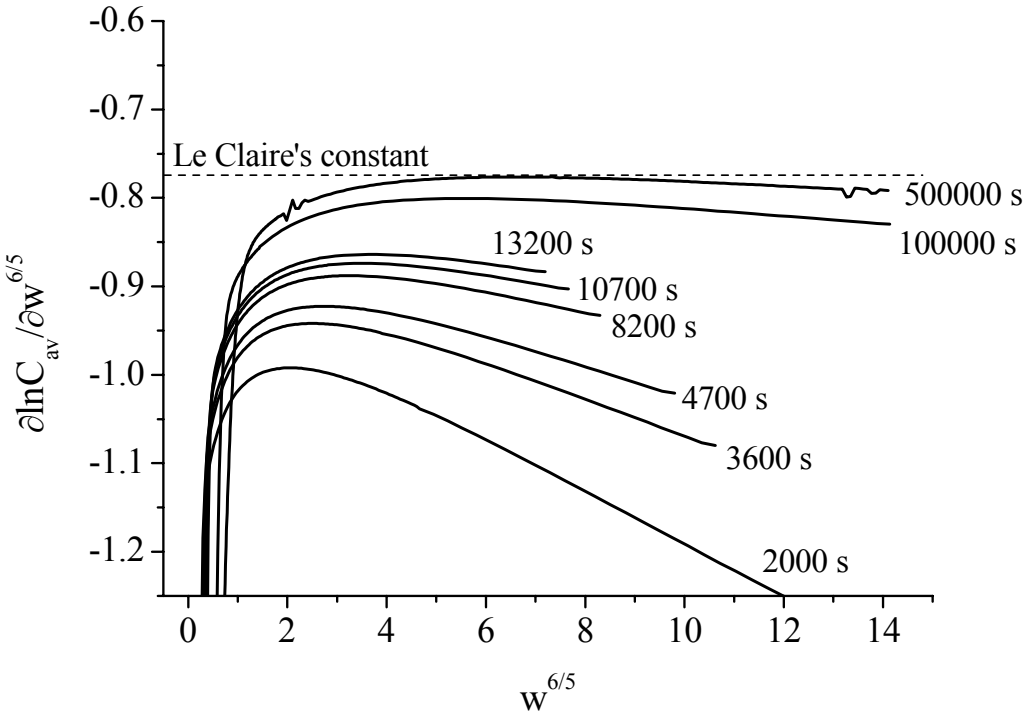
-0.6
-0.7
-0.8
-0.9
-1.0
-1.1
-1.2
Le Claire's constant
500000 s
100000 s
13200 s
10700 s
8200 s
4700 s
3600 s
2000 s
0
2
4
6
8
10
12
14
$\partial \ln C_{av} / \partial w^{6/5}$
$w^{6/5}$

c)

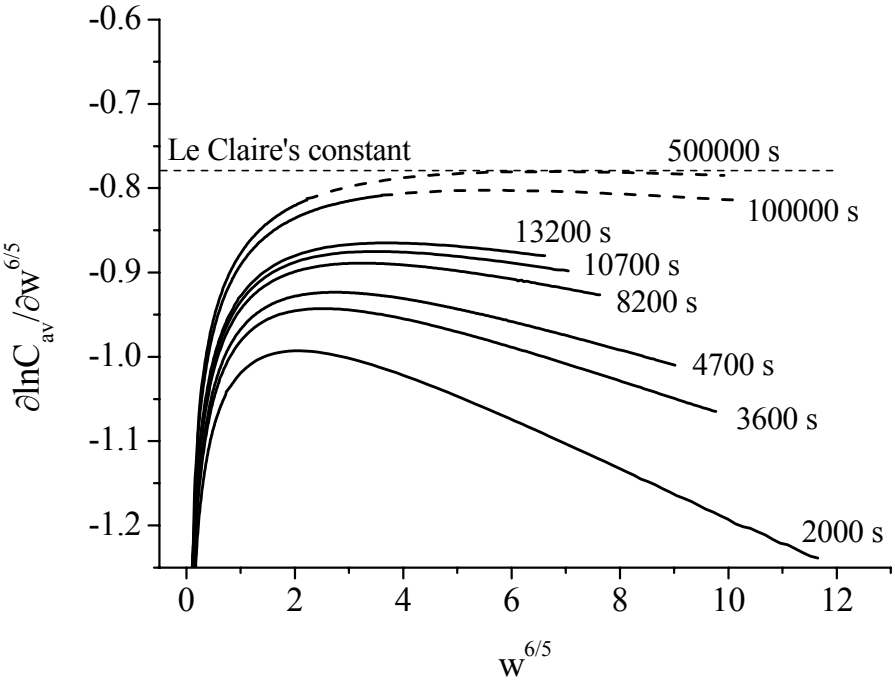

d)

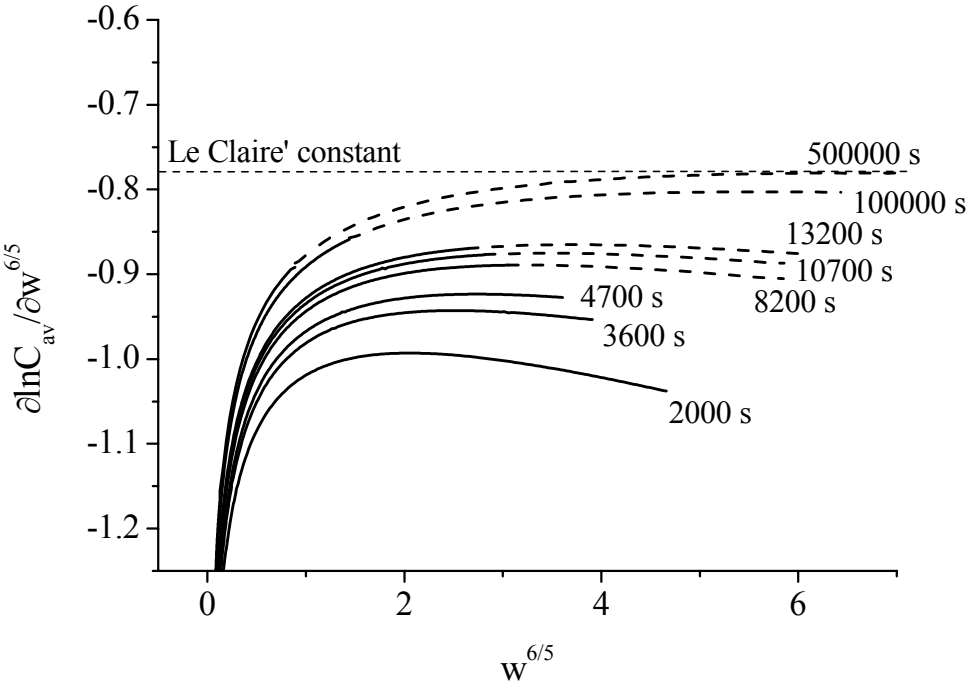

Fig. 3.13 Variation of the derivatives $\partial \ln C_{av}/\partial w^{6/5}$ with $w^{6/5}$ for a) $\Delta = 10^2$, b) $\Delta = 2.2 \cdot 10^4$, c) $\Delta = 10^3$ and d) $\Delta = 10^5$ at different diffusion times. Le Claire's constant is also indicated. The dashed curves were obtained by increasing the length of the sample and indicate restriction due to this finite length.

All the points discussed so far give a clear explanation of how the errors arise when extremely small diffusion lengths come into play. These situations very likely occur in nanomaterials with very small grains. As D_{gb} needs to be obtained, such an error analysis must be done as far as experimental evaluation is concerned. However, it is difficult to take account all the effects observed in the preceding sections. Obviously, improved procedures to deduce D_{gb} are necessary.

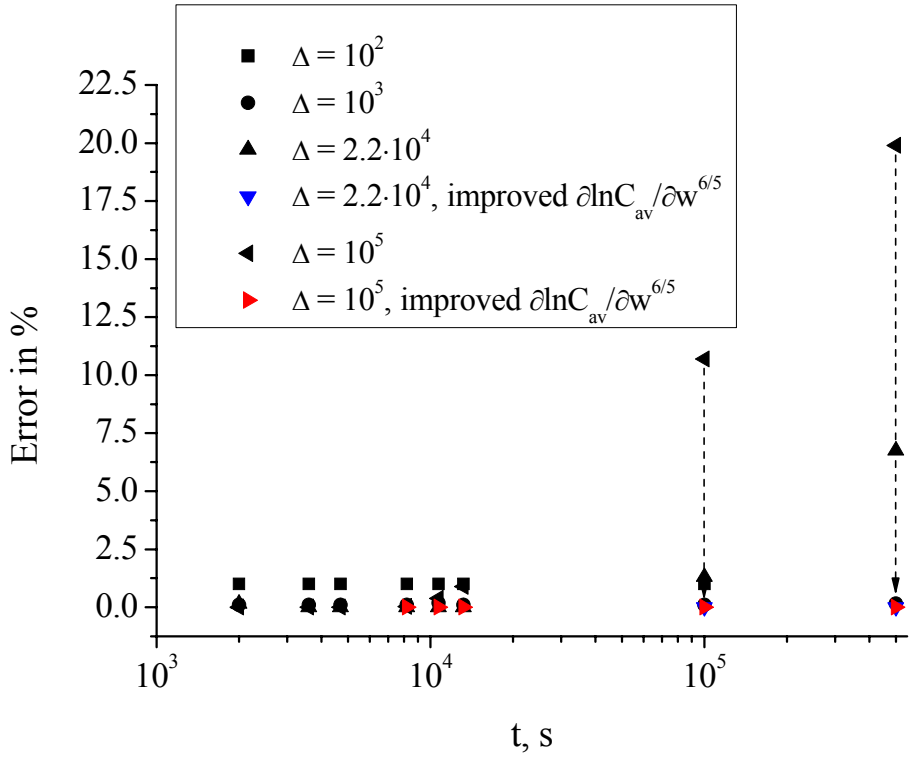

Fig. 3.14 Errors in determining D_{gb} calculated by putting both maxima on $y^{6/5}$ and $w^{6/5}$ into the original Le Claire expression. The dashed arrows show how the error is reduced after using the improved derivative.

3.4 Discussing new procedures for finding the grain boundary diffusivity

3.4.1 An analytical expression for $\partial \ln C_{av}/\partial w^{6/5}$ at the maximum

First of all, a very useful expression can be suggested for the derivative $\partial \ln C_{av}/\partial w^{6/5}$. Plotting the maxima found in the preceding section from the dependences $\partial \ln C_{av}/\partial w^{6/5} =$

$f(w^{6/5})$ as functions of another dimensionless parameter α (Eq. (1.9d)), it was observed that they almost linearly dependent on α (fig. 3.15). A small curvature, seen in this figure, cannot introduce a large error. As it can be expected, and was mentioned above, the maxima for $\Delta > 10^2$ almost coincide, and only the result for $\Delta = 10^2$ is slightly different from all the others. Despite that fact, one can see the slopes of all of the lines being the same. The values of α vary from 0.02 at longer times to 0.32 at shorter times. The large values of α as 0.32 can be attributed to the so-called B_1-regime [Mis95], [Mis92a] – the transition between the B- (B_2- or B_2'-) and C- regimes. This regime can be relevant for discussion here. Consequently, the result in fig. 3.15 shows that the B_1-regime especially important for the cases of shallow penetrations.

Fitting the lines shown in fig. 3.15 to a straight line yields the following expression

$$\frac{\partial \ln C_{av}}{\partial w^{6/5}} = -0.77 - 0.71\alpha\,, \tag{3.1}$$

neglecting the difference which exists between the line for $\Delta = 10^2$ and the others. This expression is very helpful (at least in the range of α used) since one can simply estimate the value of α, which only requires D_g to be known. According to fig. 3.15, $\alpha > 0.02$ requires Eq. (3.1) to be used to find the derivative $\partial \ln C_{av}/\partial w^{6/5}$ properly. If it is not the case, Le Claire's constant should be put into the original expression for the δD_{gb} – product.

According to what was discussed before, there are some cases when the derivative taken at the maximum also leads to significant errors (this is concerned only the derivative on w, if the length of the sample is too short to arrive exactly at the maximum). On the other hand, by plotting the derivative $\partial \ln C_{av}/\partial y^{6/5}$ it can be found out whether or not the maximum is reached. For the accurate determination of D_{gb}, it is suggested to increase the penetration depth (if not the length of the sample) until the maximum is reached despite these errors. This is, because the value of $\partial \ln C_{av}/\partial w^{6/5}$ at the depth corresponding to the length of the sample is impossible to find. Table 2.1 compares the values of $\partial \ln C_{av}/\partial w^{6/5} = f(w^{6/5})$ at the maximum taken from the calculated dependences (fig. 3.13) with those found by using Eq. (3.1).

It should be emphasized that Szabo *et al.* [Sza90] in their discussion of how to find the segregation coefficient (s) and D_{gb} separately, observed deviations of the apparent parameters from the true ones if α increases. The explanation of this effect is given here and, moreover, an improved procedure to deduce D_{gb} is suggested.

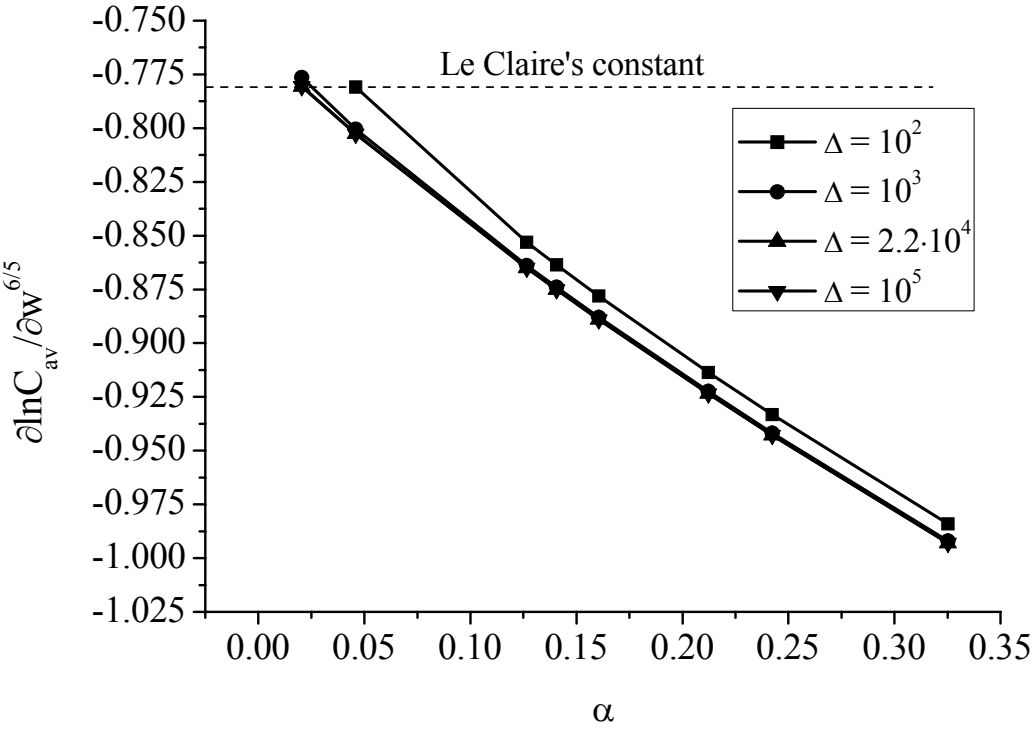

Fig. 3.15 Maxima of the dependences $\partial \ln C_{av}/\partial w^{6/5} = f(w^{6/5})$ plotted against the dimensionless parameter α for different ratios Δ.

Table 3.1 A comparison of the derivatives at the maximum found by using calculated dependences and Eq. (3.1) for $\Delta = 2.2 \cdot 10^4$.

t, s	$\partial \ln C_{av}/\partial w^{6/5} = f(w^{6/5})_{true}$	$\partial \ln C_{av}/\partial w^{6/5} = f(w^{6/5})_{Eq.\ 2.\ 1}$
2000	-0.99	-1.00
3600	-0.94	-0.94
4700	-0.92	-0.92
8200	-0.89	-0.88
10700	-0.87	-0.87
13200	-0.86	-0.86
100 000	-0.80	-0.80
500 000	-0.78	-0.78

3.4.2 The reason of observing a constant value for $\partial \ln C_{av}/\partial w^{6/5}$. Discussing procedures used in the literature

It is believed that there are certain cases when the exact Whipple's solution can be transformed to a simpler mathematical form. These cases have been for the first time introduced by Whipple [Whi54] and Le Claire [Cla63] and were explicitly discussed later in the book of Kaur *et al.* [Kau95]. The origin of those transformations lies in a fact that the ratio of diffusivities (Δ) can be very large, typically, of the order of 10^5 or so for metals. The expression for C_g (used in the cited paper of Le Claire) then reads:

$$C_g(\eta,\xi,\beta) = \operatorname{erfc}\left(\frac{\eta}{2}\right) + \frac{\eta}{2\pi^{1/2}}\int_1^{\infty}\frac{d\sigma}{\sigma^{3/2}}\exp\left(-\frac{\eta^2}{4\sigma}\right)\operatorname{erfc}\left[\frac{1}{2}\left(\frac{\sigma-1}{\beta}+\xi\right)\right]. \qquad (3.2)$$

The meaning of the dimensionless quantities η and ξ was given in chapter I (Eqs. (1.9b) and (1.9c)). By comparing with Eq. (1.9a) the upper limit Δ is replaced by infinity, and the term $\left(\frac{\Delta-1}{\Delta-\sigma}\right)^{1/2}$ under the complementary error-function is simply ignored. After Le Claire, the same transformation was applied by Chung and Wuensch [Chu96a], [Chu96b], and it is important to discuss this once more in order to prevent possible errors. As it has been explained [Kau95], the approximation $\Delta \to \infty$ may be used when $\beta << \Delta$ with β remaining finite. In the present study β was varied from 2 ($\Delta = 10^2$, t = 100000 s) to 32518 ($\Delta = 10^5$, t = 2000 s), always being smaller than Δ. Strictly speaking, the ratio Δ/β is 50 at longer times and only 3 at shorter times for all Δ used. Additionally, η (Eq. (1.9b)) varies from 41 to 650 in all the calculations in the present study. These values of η are smaller than Δ, except for Δ as small as 10^2. Since η is weighted by the diffusion length L_g, the ratio y/L_g is exactly of the order of several hundreds or smaller; otherwise extremely deep penetrations come into play. Unrealistic situations, when $\eta >> \Delta$ were supposed by Le Claire when suggesting Eq. (3.2). On the other hand, such an approximation allows the contribution of bulk diffusion to be neglected, and Le Claire transformed Eq. (3.2) to a special mathematical form for C_{av}, neglecting the bulk diffusion part. One can also think of this approximation in terms of w. If η is much larger than Δ which itself is much larger than β, then w increases to values of tens or even hundreds. Nevertheless, the maximum of $\partial \ln C_{av}/\partial w^{6/5}$ lies in the region of w from 2 to 6 and not larger. In fig. 3.16 two derivatives are shown, calculated under condition $\beta < \Delta$. The

first of them was obtained by using a convenient mathematical form to better integrate Eq. (3.2), published in [Kau95], excluding bulk diffusion. The second one was found by using the same mathematical form, taking into account bulk diffusion. The equation used for integration is

$$C_{av} = \operatorname{erfc}\left(\frac{w\beta^{1/2}}{2}\right) + \frac{4\left(D_g t\right)^{1/2} w}{L\pi^{1/2}} \int_0^{\beta^{1/2}} \exp\left(-\frac{w^2\tau^2}{4}\right) \left[\begin{array}{l} \frac{1}{\pi^{1/2}} \exp\left\{-\frac{1}{4}\left(\frac{1}{\tau^2}-\frac{1}{\beta}\right)\right\} \\ -\frac{1}{2}\left(\frac{1}{\tau^2}-\frac{1}{\beta}\right) \operatorname{erfc}\left\{\frac{1}{2}\left(\frac{1}{\tau^2}-\frac{1}{\beta}\right)\right\} \end{array}\right] d\tau, \qquad (3.3)$$

where τ is a new integration variable related to σ through $\tau = \left[\left(\frac{\Delta-\sigma}{\Delta-1}\right)\frac{\beta}{\sigma}\right]^{1/2}$; L is the width of the sample or the distance over which C_g is averaged. The difference between Eq. (3.3) and the one originally suggested in [Kau95] lies in the use of bulk diffusion part. Comparison of both equations shows that the maximum is not influenced by neglecting bulk diffusion (fig. 3.16, dashed lines). This again confirms that the bulk part is confined within a very tiny region, what is also shown in fig. 3.10. So the maximum lies far enough from the bulk part and corresponds only to the GB diffusion. Interestingly, Eq. (3.3) was integrated successfully by using MatLab without any serious numerical problems. One may conclude here that, in principle, bulk diffusion may be excluded but not because $\eta >> \Delta$ which is an unrealistic condition. Interestingly, the maximum of the calculated derivatives is slightly higher than Le Claire's constant.

More important is another condition, *viz.* $\beta << \Delta$. The ratio $\Delta/\beta = 50$ leads to Le Claire's constant, according to the results of the present study. Comparing this with what was discussed by Chung and Wuensch [Chu96a], $\Delta/\beta \geq 50$ looks much more realistic. They used the condition Δ/β ($\approx 2L_g/\delta$) $\geq 10^3$ in order to apply $\Delta \to \infty$. In this case $\beta \approx \Delta/10^3$. For small ratios Δ, say 10^2 or 10^3, the condition is never fulfilled, giving the values smaller or equal than 1. This would mean that the measurements on small angle boundaries could not be evaluated.

Continuing the discussion started in [Kau95] with respect to the reasons leading to $\Delta \to \infty$, the erfc-term in Whipple's solution (Eq. (1.9a)) was plotted against σ for two extreme cases: $\Delta = 10^5$ and $\Delta = 10^2$ (fig. 3.17). The diffusion time (t) was varied from 2000 s to 500000 s not only because exactly these times were used in the present study, but also

because these cover the values of β which can be met in the measurements. The values of $\beta \geq \Delta$ would mean $L_g \leq \delta$, what corresponds to the type-C diffusion kinetics. Consequently, another criterion for the C-regime is $\beta > \Delta$, which is the same as $L_g < \delta$ and leads to complex C_g. Otherwise, L_g is larger than δ, and the B-regime becomes responsible for the diffusion process, regardless we refer to the classical B-regime or B_2, B_2', or B_1.

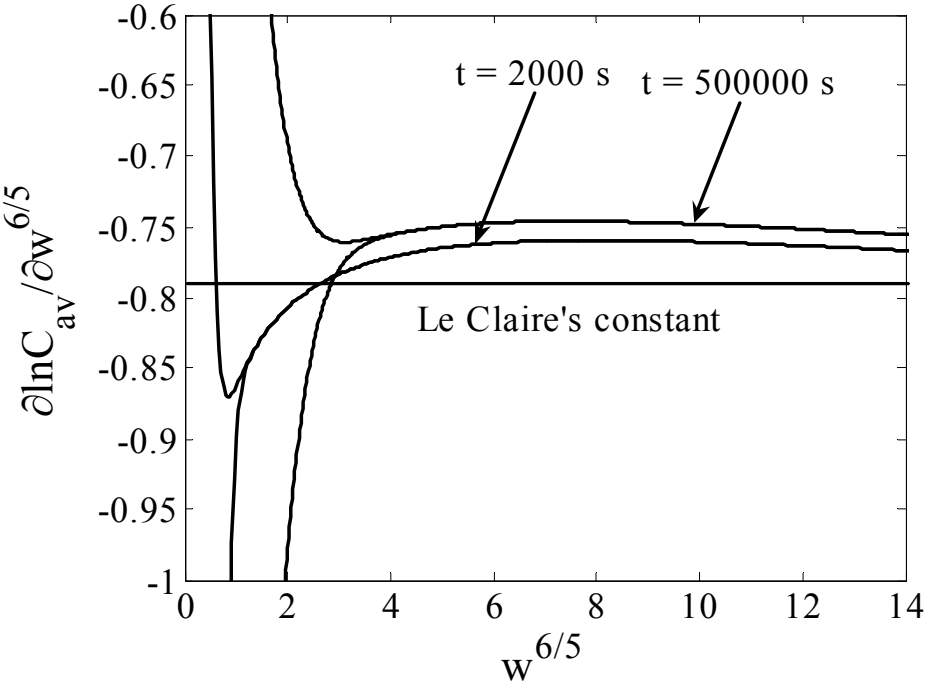

Fig. 3.16 Variation of the derivatives with $w^{6/5}$ calculated for $\Delta = 10^2$ by using Eq. (3.3) excluding (dashed curves) and including (solid curves) the bulk diffusion part.

Appreciable values of the erfc-term are possible, if β is close to Δ. In these cases the upper limit of integration should be exactly Δ. If β decreases, the upper limit can be taken smaller and at t = 500000 s it can surely be replaced by infinity (fig. 3.17). In fact, it is a very restricted region of β, when $\Delta \to \infty$ may be used for nanomaterials. The restriction is defined by L_g, because increase of t leads finally to the A′-regime as it is the case for $\Delta = 10^5$ with the average grain size of 50 – 100 nm or so (fig. 1.5d). This is the typical situation for nanomaterials when we proceed to the A-type regimes at large β. The new criterion for using $\Delta \to \infty$, suggested in the present study, is that α should be smaller than 0.02. Interestingly, if it is not taken into account, the integration of Eq. (3.3) gives Le Claire's constant, even if $\alpha >$ 0.02 (fig. 3.18). This, of course, can be misleading. This is the aim of the experiment to find β, while α can be estimated, knowing D_g. Consequently, the analysis in terms of α is more convenient and allows one to make all necessary conclusions.

a)

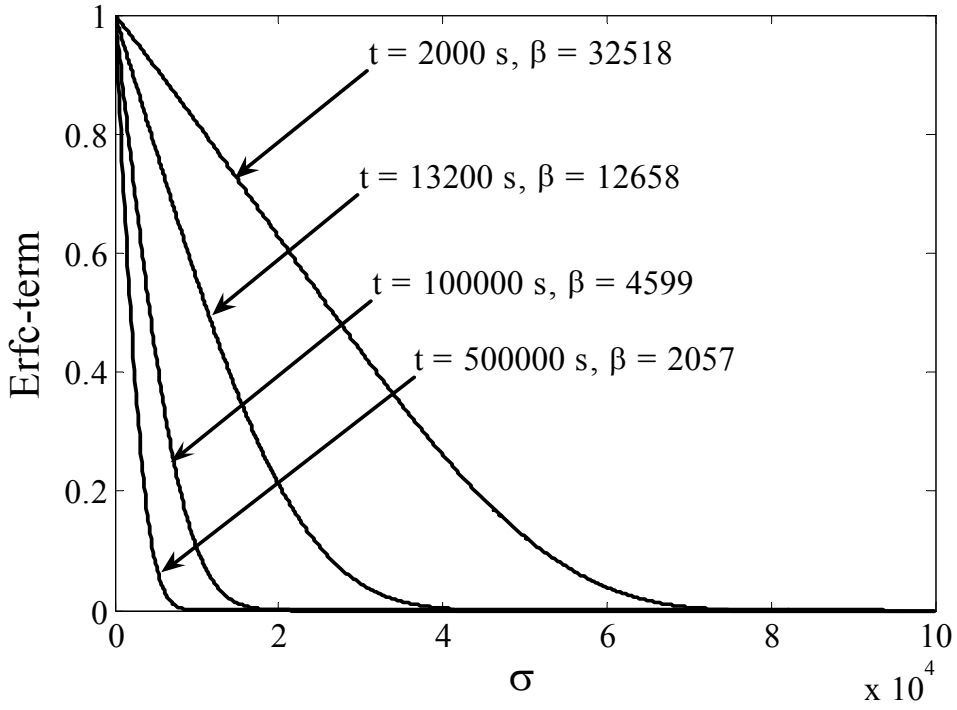

b)

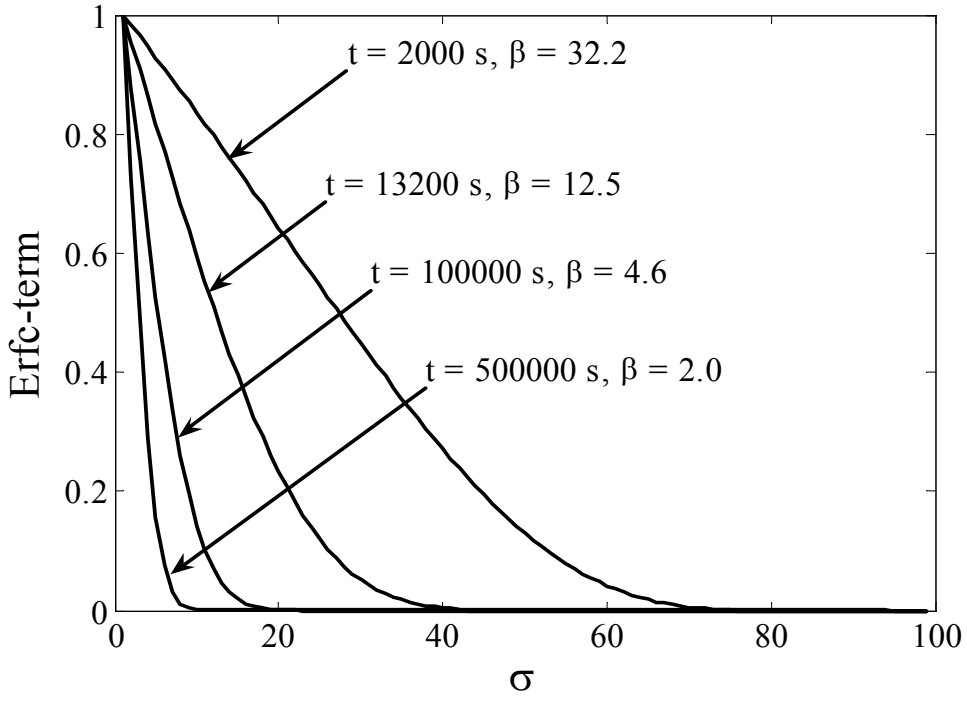

Fig. 3.17 The term erfc[…] taken directly from Whipple's solution (Eq. (1.9a)) is calculated at $\xi = 0$ for $\Delta = 10^5$ a) and $\Delta = 10^2$ b).

a)

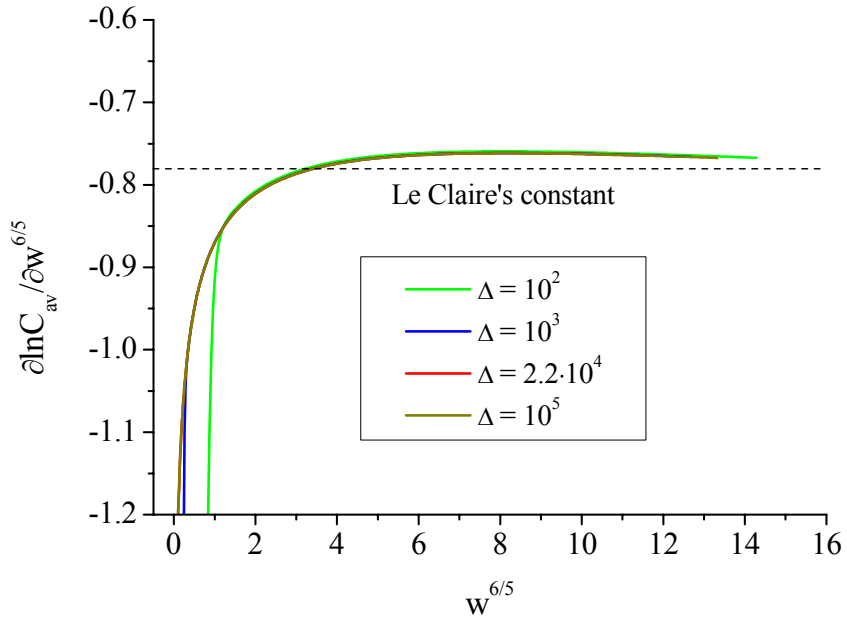

b)

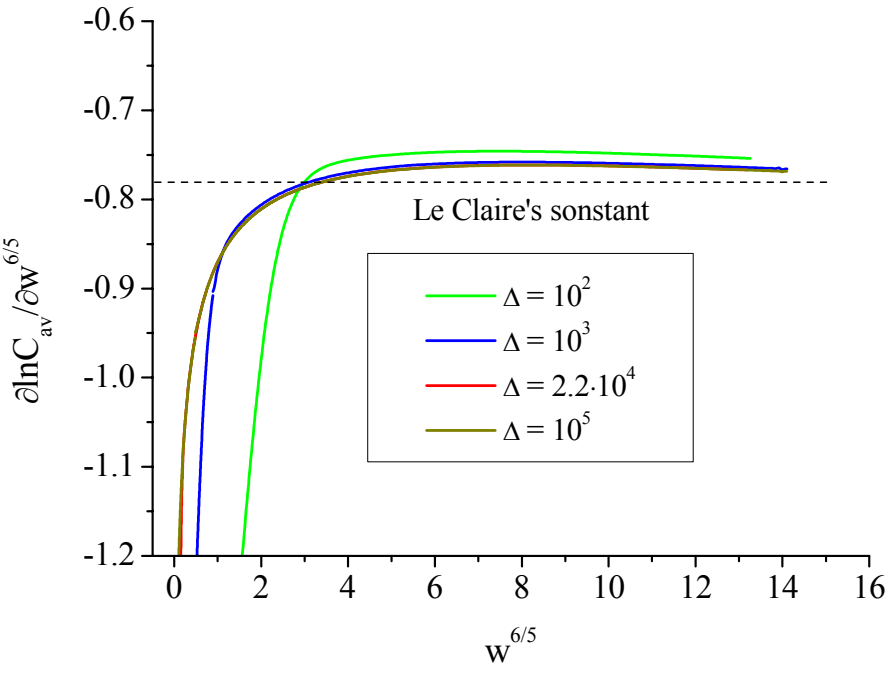

Fig. 3.18 Variation of the derivative $\partial \ln C_{av}/\partial w^{6/5}$ as a function of $w^{6/5}$ calculated by using Eq. (3.3) for different ratios Δ at t = 2000 s a) and t = 500000 s b).

An additional and important comment is that similar results can also be obtained, say for $\Delta = 10^2$, if in the exact Whipple solution $\Delta = 10^5$ (the upper limit of integration) is used instead of Δ with β corresponding to $\Delta = 10^2$. This is, of course, an artificial point, which is nothing but only a mathematical trick to get to Le Claire's constant, because the range of varying σ is increased in this case. In this sense the following question arises. Is the result obtained for a very short time correct under these conditions? Probably, it would be enough to increase the range for σ. The answer is very nicely given by comparing the exact Whipple solution with the result of FEM. By using numerical method to integrate Fisher's system (Eq. (1.6)), one observes the solution independent of Whipple's solution and, consequently, of $\Delta \to \infty$. The corresponding result is discussed in chapter IV (fig. 4.1). Here it is only important to mention that the results of both integrations coincide within a very small error even at 2000 s.

3.4.3 On important dependences for finding the grain boundary diffusivity

Summarizing the previous sections, the following procedure could be suggested for nanomaterials: 1) Measure the diffusion profile and determine D_g by simply fitting the near surface part to the complementary error-function solution or Gaussian function depending on boundary conditions. 2) Plot the derivative of the measured diffusion profile and identify its maximum, $(\partial \ln C_{av}/\partial y^{6/5})_{max}$ (it is recommended to reach this maximum). 3) Calculate the parameter α. 4) If $\alpha > 0.02$, use Eq. (3.1) to find the derivative $(\partial \ln C_{av}/\partial w^{6/5})_{max}$ and put the derivatives into Eq. (1.14), or if $\alpha < 0.02$ use the standard Le Claire constant. The disadvantage of this procedure is in fact, that plotting the derivative can be a serious problem for the experimental profile due to, for example, scattering of the experimental points [Kow00]. An alternative procedure which further improves the determination of D_{gb} and is more sufficient for ionic materials (as it will be shown in chapter V) is discussed now.

As far as the maximum is responsible for the accuracy of determined diffusion coefficient D_{gb}, it would be better to find the derivative at the maximum as accurately as possible. It seems to be the only possibility to find D_{gb} accurately. Because of this, it would be particularly interesting to analyze how the position of the maximum depends on t. In fig. 3.19 the positions for different Δ are plotted as functions of t on the logarithmic scale. It is very likely that the positions are linearly dependent on t on the logarithmic scale, what is very well seen for smaller ratios Δ. The points for $\Delta = 2.2 \cdot 10^4$ and 10^5 at long t are affected by the finite length of geometrical model (500 nm), reflecting that the necessary maximum is not reached.

That is why, the maxima for these large ratios Δ were taken at one point of 500 nm, beginning from 13200 s for $\Delta = 10^5$ and 100000 s for $\Delta = 2.2 \cdot 10^4$. The following relationship for $y^{6/5}$ at the maximum is found:

$$\log(y_{max}^{6/5}) = \log(K) + H \cdot \log(t)$$

or (3.4)

$$y_{max}^{6/5} = K \cdot t^H,$$

where t is as usually the diffusion time, K is a normalizing coefficient which depends on Δ and, in general, on D_g and D_{gb}. However, the most useful information comes from the parameter H which is found out to be independent of D_g and D_{gb}, at least in the considered range of parameters. The parameter H determines the slope of the lines in fig. 3.19 and allows one to know t needed to reach the maximum, if the diffusion profile once measured is too shallow. This power law is not surprising since it reflects the typical diffusion property – dependence as a power law on t. In order to realize the long times (10^7 s – 10^{10} s) for large ratios Δ, the width as well as the length of the sample was increased (fig. 3.20), and Eq. (3.2) was integrated since β is much smaller than Δ. Consequently, the parameter H was determined by fitting the lines in figs. 3.19 and 3.20 to a straight line and is summarized in table 3.2. The perfect linear dependences were observed for short and very long times (red lines, reflecting the fitting in fig. 3.20, show this very clearly). Comparing the results of integration of the exact Whipple solution and Eq. (3.2) at t = 500000 s shows that the latter slightly overestimates the maximum positions (not shown here). The exact Whipple solution could not be integrated at so high t properly leading to very strong numerical instabilities. The dependencies in fig. 3.20 are characterized by a nonlinearity which is also seen for $\Delta = 10^3$ and 10^2 in fig. 3.19. The width of 5157 nm (~ 5.16 μm) was applied for $\Delta = 10^5$, what demonstrates that a micrometer regime is already relevant here. However, this gives huge diffusion times which will never be realized in the experiments at least for the parameters D_g, D_{gb} used in the present study; however the temperature can be increased. More importantly, the slopes for all Δ used are very well comparable for short t (table 3.2). In these calculations the β – parameter was varied up to ~10 – 15 for all Δ. The most reasonable value of H is 0.6, because it suggests that $y_{max} \sim t^{1/2}$ – the expected dependence. As the diffusion time grows up, the process slowly develops with time in a comparison with short t giving rise to the nonlinearity in figs. 3.19 and 3.20 (this can be the second reason explaining the effect of nonlinearity discussed in the preceding sections).

A similar behavior was observed for the maximum of the derivatives. When plotting the absolute values of maxima for relevant ratios Δ from t = 2000 s up to 500000 s, straight lines arise on the logarithmic scale (fig. 3.21). Again and importantly, similar slopes were observed for all the ratios Δ. In the dependence for the position of the maximum the values K are Δ-dependent, and to analytically calculate the position one needs to know this parameter. However, the most important is the maximum which can directly be put into Eq. (1.16). The general expression for the lines in fig. 3.21 is represented as follows:

$$\log\left|\frac{\partial \ln C_{av}}{\partial y^{6/5}}\right|_{max} = \log(A) + B\cdot\log(t), \tag{3.5}$$

where B is the slope of the dependence $\log\left|\frac{\partial \ln C_{av}}{\partial y^{6/5}}\right|_{max} = f\left(\log(t)\right)$, A is the parameter which is Δ-dependent and also depends on t. In table 3.3 the values of the slopes are summarized for various Δ. These are very close to each other, indicating that single slope of approximately –0.34 may be used when calculating the derivative $-\partial \ln C_{av} / \partial y^{6/5}$ at the maximum, at least for $D_g = 2.95\cdot10^{-4}$ nm^2/s. This conclusion is not very much different from the analysis performed by Atkinson and Taylor [Atk79], since they supposed that the gradient $-\partial \ln C_{av} / \partial y^{6/5}$ should be proportional to $t^{-0.3}$. However, an analytical relation to find the slope was not suggested.

All the quantities in Eq. (3.5) do not bear enough information on the diffusion coefficients. These quantities are dependent on the parameters and vary with both Δ and absolute values of D_g and D_{gb}. In this form Eq. (3.5) is difficult to use for finding Δ. However, it could be particularly important, since in many cases the measured diffusion profile can be influenced by additional processes accompanying diffusion of a solute in the material. Even though the quantities A and B are known, it is unclear how to relate them to Δ. If the quantity B is supposed to be a constant, there should be a relation between the quantities A and Δ. The later comes from the fact that the lines in fig. 3.21 are shifted up with increased Δ.

Consequently, the values of A found by fitting the functions in fig. 3.21 to the straight line were plotted against Δ. The corresponding result shown in fig. 3.22 suggests that there is a linear dependence of log(A) on log(Δ) also on the logarithmic scale. This is a particularly important result, because it directly relates the slope (the maximum of the derivative) of the diffusion profile with the ratio Δ. According to this plot and in the fashion of Eq. (3.5) log(A) can be found by using

$$\log(A) = \log(C) + F \cdot \log(\Delta). \tag{3.6}$$

In this equation the quantity C can be different depending on D_g and t, and finally, the general expression for the slope is

$$\log\left|\frac{\partial \ln C_{av}}{\partial y^{6/5}}\right|_{max} = \log(C) + F \cdot \log(\Delta) + B \cdot \log(t)$$

or (3.7)

$$\left|\frac{\partial \ln C_{av}}{\partial y^{6/5}}\right|_{max} = C \cdot \Delta^F \cdot t^B$$

All the dependencies (Eqs. (3.5) and (3.6)) reflect the fact that the maximum of derivative follows a single law when increasing the ratio Δ or time t. Further details on using Eq. (3.7) will be discussed in chapter V.

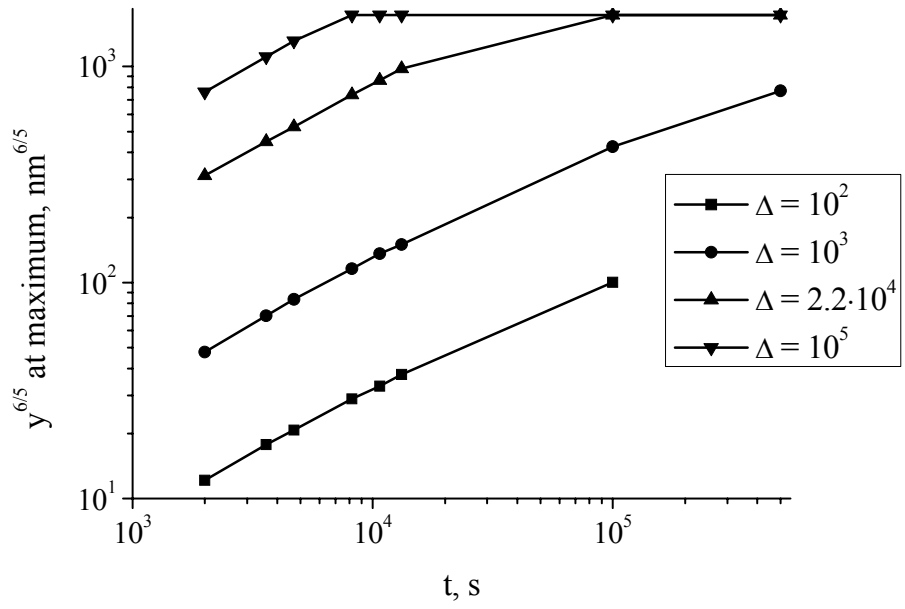

Fig. 3.19 Variation of $y^{6/5}$ taken at the maximum of the derivatives $\partial \ln C_{av}/\partial y^{6/5}$ with t for different Δ on the logarithmic scale. The length of the geometrical model is 500 nm.

Table 2.2 Different slopes H varying t ($y_{max}^{6/5}$).

Δ	H(t)		
	$2\cdot10^3$ s ≤ t ≤ $1.32\cdot10^4$ s	$1\cdot10^5$ s ≤ t ≤ $2.1\cdot10^6$ s	$2.1\cdot10^6$ s ≤ t ≤ 10^{10} s
10^2	0.59	0.53 (up to $1\cdot10^5$ s)	-
10^3	0.58	0.50 (up to $5\cdot10^5$ s)	-
$2.2\cdot10^4$	0.60	0.42 (0.50)	0.29
10^5	0.61	0.42	0.30

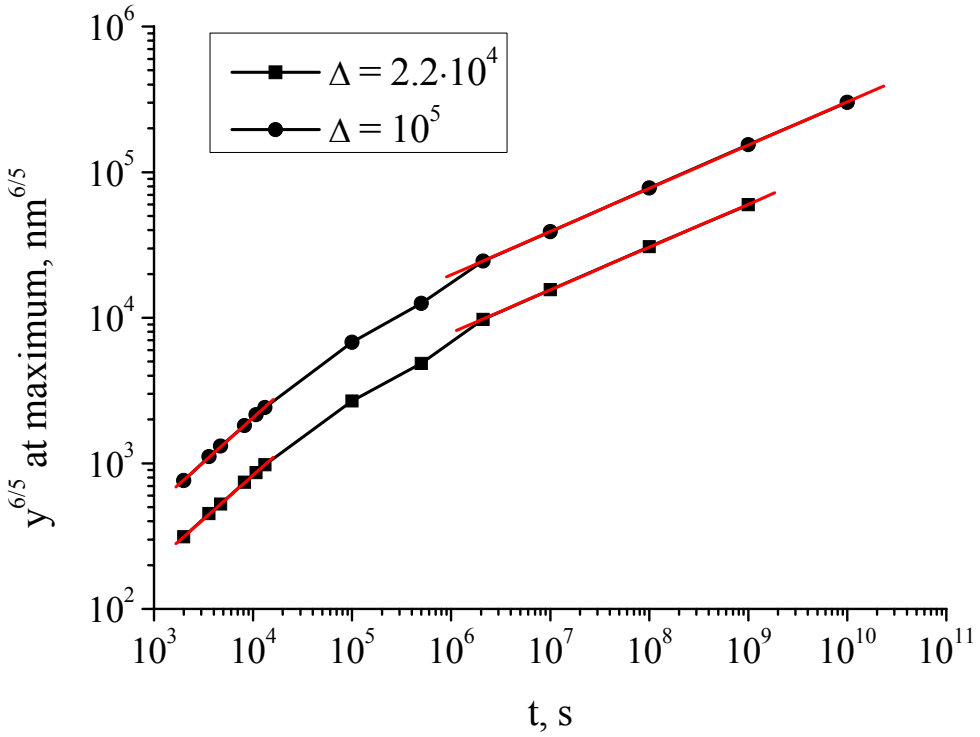

Fig. 3.20 Variation of $y^{6/5}$ taken at the maximum of the derivatives $\partial \ln C_{av}/\partial y^{6/5}$ with t for different Δ on the logarithmic scale. The width and the length of the geometries were increased to reach small values of β: the length of about 40 000 nm is needed to integrate Eq. (3.2) for $\Delta = 10^5$ at $t = 10^{10}$ s. Red lines correspond to the fitting.

Table 3.3 The values of the slope B for various Δ ($D_g = 2.95\cdot10^{-4}$ nm^2/s).

Δ	B
10^2	-0.32
10^3	-0.33
$2.2\cdot10^4$	-0.34
10^5	-0.36

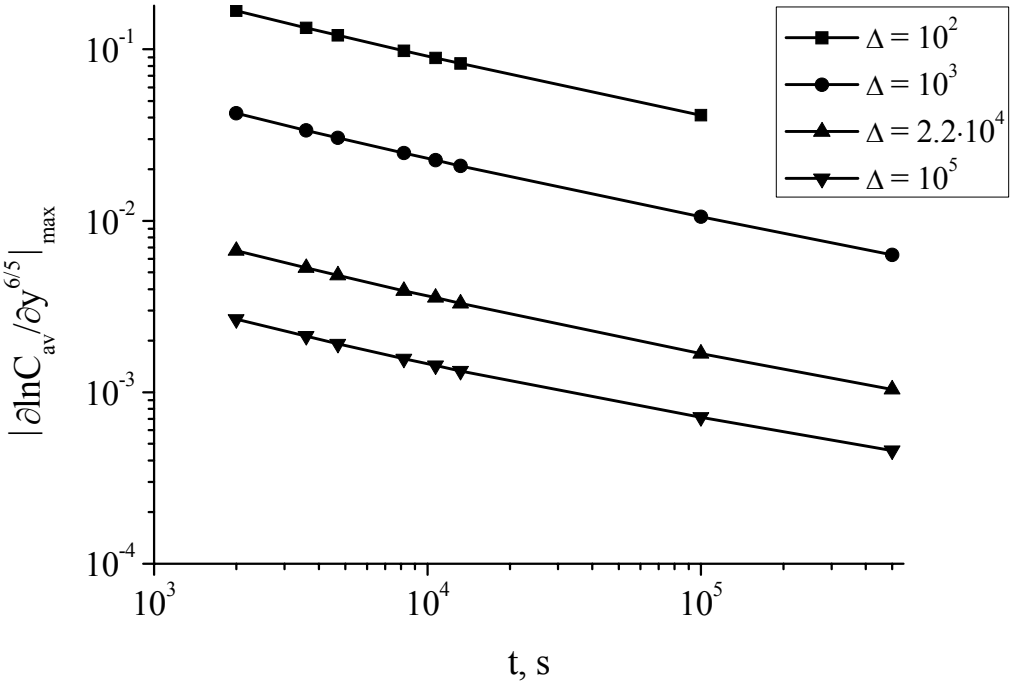

Fig. 3.21 Variation of the modulus of the maximum with t for different Δ. The result is performed on the logarithmic scale.

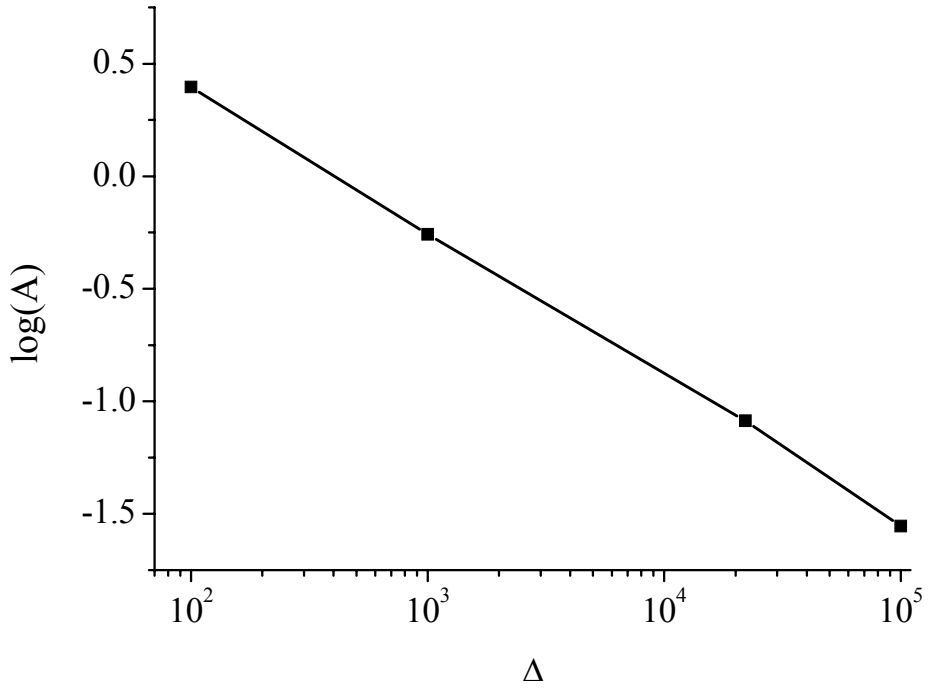

Fig. 3.22 Variation of log(A) in Eq. (3.5) with Δ.

Summary

It is shown that the nonlinearity of the diffusion profile $\ln C_{av} = f(y^{6/5})$ has to be analyzed, especially at short diffusion times. The maximum of the diffusion profile can be used to find the GB diffusivity accurately under such conditions. This maximum corresponds to the diffusion kinetics which is relevant under certain conditions. The use of Le Claire's relation requires type-B kinetics, and the maximum reflects that situation. Application of Le Claire's constant of 1.322 leads to errors at very short diffusion times. In order to improve the determination of the GB diffusivity, an equation is suggested to find the derivative $(\partial \ln C_{av}/\partial w^{6/5})$ at the maximum. The improved procedure is explained in detail. Additionally, new dependences are derived on the basis of integrations of the exact Whipple solution for the maximum value of $(\partial \ln C_{av}/\partial y^{6/5})$ and its position. For the dependence of the gradient $(\partial \ln C_{av}/\partial y^{6/5})$ at the maximum the quantity B is found to be ~-0.34. The value of the gradient at a certain diffusion time can be directly used in the Le Claire relation, if the quantities F and C are known.